

1 **Title: Comparative brain structure and the neural network features of cuttlefish and**  
2 **squid**

3

4 **Authors:** Wen-Sung Chung<sup>1,3,\*</sup>, Alejandra L. Galan<sup>1</sup>, Nyoman D. Kurniawan<sup>2</sup>, N. Justin  
5 Marshall<sup>1</sup>

6 **Affiliations:**

7 <sup>1</sup> Queensland Brain Institute, The University of Queensland, St Lucia, QLD 4072, Australia

8 <sup>2</sup> Centre for Advanced Imaging, The University of Queensland, St Lucia, QLD 4072,  
9 Australia

10 <sup>3</sup> Lead contact

11 \* Correspondence (w.chung1@uq.edu.au)

12

### 13 **Abstract**

14 Cuttlefishes, like their octopus cousins, are masters of camouflage by control of body  
15 pattern and skin texture to blend in with their surroundings for prey ambush and threat  
16 avoidance. Aside from significant progress on the cuttlefish visual perception and  
17 communication, a growing number of studies have focused on their behavioural neurobiology  
18 and the remarkably rapid and apparently cognitively complex reactions to novel challenges  
19 such as spatial learning to solve maze tasks and vertebrate-like cognitive capabilities (e.g.  
20 object recognition, number sense and episodic-like memory). Despite intense interest of  
21 cuttlefish, much of our knowledge of its neuroanatomy and links to behaviour and ecology  
22 comes from one temperate species, the European common cuttlefish, *Sepia officinalis*. Here  
23 we present the first detailed comparison of neuroanatomical features between the tropical  
24 cuttlefish and squid and describe differences in basic brain and wiring anatomy using MRI-  
25 based techniques and conventional histology. Furthermore, comparisons amongst nocturnal  
26 and diurnal cuttlefish species suggest that the characteristic neuroanatomical features infer  
27 interspecific variation in visual capabilities, the importance of vision relative to the less  
28 utilised chemosensory system and clear links with life modes (e.g. diurnal vs nocturnal),  
29 ecological factors (e.g. living depth and ambient light condition) as well as to an extent,  
30 phylogeny. These findings link brain heterogeneity to ecological niches and lifestyle, feeding  
31 hypotheses around evolutionary history and provide a timely, new technology update to older  
32 literature.

33 **Introduction**

34 Cuttlefish, squid and octopus are the three groups of coleoid cephalopods exhibiting  
35 diverse adaptations in body form, life modes and behavioural repertoires. This is reflected in  
36 the underlying nervous system (Nixon and Young, 2003, Hanlon and Messenger, 2018).  
37 While the fourth extant group of cephalopods, Nautilus, has an obvious external shell, gas-  
38 filled and used for floatation, octopus and squid have lost almost all remnants of this ancient  
39 feature and may therefore inhabit a broad range of ocean depths (0-6000 m) (Jereb and Roper,  
40 2010, Jereb et al., 2014). The cuttlefish possess an internal chambered cuttlebone that, while  
41 giving internal strength, is also controllably gas-filled and therefore the risk of implosion  
42 limits their living depth to above 400m. Interestingly, for unknown reasons, they also have a  
43 limited geographic distribution (high diversity in the Indo-Pacific but absence in the  
44 Americas and polar regions) (Sherrard, 2000, Jereb and Roper, 2005, Lu and Chung, 2017).  
45 The cuttlebone allows buoyancy control by adjustment of the ratio between air and liquid and  
46 cuttlefish can therefore hover in the water column or bury themselves in sand to hide. This  
47 hovering, usually close to the benthos, is in contrast to the continual swimming activity of  
48 squid and the almost exclusively benthic existence of coastal octopus (Denton and Gilpin-  
49 Brown, 1961, Hanlon and Messenger, 2018).

50 A growing number of *in situ* observations of cuttlefish species show that they are not  
51 solitary, as are most of the species of neritic octopuses and also not as social as schooling  
52 species of squid (Hanlon and Messenger, 2018, Lu and Chung, 2017). Cuttlefish may  
53 therefore have a partially social life and are known to aggregate, sometimes in large numbers,  
54 for breeding on a seasonal basis (e.g. European common cuttlefish, *Sepia officinalis*;  
55 Broadclub cuttlefish, *Sepia latimanus*; Australian giant cuttlefish, *Sepia apama*) (Norman et  
56 al., 1999, Hanlon et al., 2005, Yasumuro et al., 2015, Drerup and Cooke, 2021).

57 Cuttlefishes, like their octopus cousins, are masters of camouflage by control of body  
58 pattern and texture to blend in with their surroundings and use this ability both for prey  
59 ambush and threat avoidance (Marshall and Messenger, 1996, Chiao and Hanlon, 2001,  
60 Hanlon and Messenger, 2018, Gonzalez-Bellido et al., 2018, Osorio et al., 2022). In fact,  
61 cuttlefish spend most of their time in very effective and totally colourblind camouflage, they  
62 may also rapidly switch colouration to emphasise their presence, produce startle threats,  
63 attract mates or indeed cheat rival males (Norman et al., 1999, Hanlon et al., 2005, Zylinski et  
64 al., 2011, Brown et al., 2012, Chung and Marshall, 2016, How et al., 2017, Alejandra et al.,  
65 2020). The ability to alter their visual appearance is driven by neurally-controlled

66 chromatophore (colours) and muscular hydrostat (papillae) systems coordinated by a set of  
67 brain lobes organised hierarchically (e.g. the simplest circuit, optic lobe (OPL) - lateral basal  
68 lobe (LB)– chromatophore lobe (Ch)) (Messenger, 2001, Gonzalez-Bellido et al., 2018).

69 The cuttlefish central nervous system (CNS) is built around a circum-oesophageal set  
70 of lobes that have expanded greatly, in part in response to their complex visual system and  
71 rapid visual-motor reactions (i.e. ballistic tentacular strike, visual communication) (Tompsett,  
72 1939, Sanders and Young, 1940, Boycott, 1961, Messenger, 1968, Chichery and Chichery,  
73 1987). The general shape of the cuttlefish CNS shows that the degree of its compactness is  
74 between octopus (compact CNS) and squid (elongated CNS) (see Fig 2.2 in Nixon and  
75 Young (2003)). Previous studies also suggested a high degree of similarity in CNS layout and  
76 underlying neural network between squid and cuttlefish, including the first of these from  
77 Cajal (1917), that initially highlighted the sophisticated visual and chromatophore systems  
78 (Sanders and Young, 1940, Boycott, 1953, Boycott, 1961, Messenger, 1968, Young, 1974,  
79 Young, 1976, Young, 1977, Young, 1979, Messenger, 1979, Budelmann and Young, 1987,  
80 Wild et al., 2015, Ponte et al., 2021). These works demonstrate the closeness of sepioids  
81 (cuttlefish) and teuthoids (squid) in spite of their long evolutionary separation (Strugnell et al.,  
82 2006, Allcock et al., 2014).

83 Early work on the organisation of the cuttlefish sensory and motor control systems was  
84 achieved through two methods: (1) Electrical stimulation of selected brain regions to detail  
85 the associating responses (Sanders and Young, 1940, Boycott, 1961, Chichery and Chanelet,  
86 1976, Chichery and Chanelet, 1978, Chichery and Chichery, 1987). (2) Comparative studies  
87 in behavioural changes and learning impairment before and after brain region ablation  
88 (Sanders and Young, 1940, Boycott and Young, 1950, Chichery and Chichery, 1987).

89 The cuttlefish CNS was divided into 5 major functional regions: (i) The vertical lobe  
90 complex located at the most dorsal part of CNS with the noticeable dome-shaped vertical  
91 lobe (VL) and the superior frontal lobe (learning and memory). (ii) A pair of optic lobes  
92 (OPL) (visual tasks). (iii) A pair of peduncle lobes (PED) (cerebellum-like lobe for visual-  
93 motor control). (iv) Supra-oesophageal mass (Higher motor centres coordinating sensory  
94 inputs and behavioural responses). (v) Sub-oesophageal mass (Lower motor centres  
95 executing movement of funnel, arms, and mantle activities). This pioneering work produced a  
96 useful model for several ensuing studies of sensory reception, learning and memory

97 (Messenger, 1973, Darmaillacq et al., 2006, Jozet-Alves et al., 2013, Yang and Chiao, 2016,  
98 Feord et al., 2020, Schnell et al., 2021b, Schnell et al., 2021a, Osorio et al., 2022).

99 Over the past two decades, a growing number of studies have focused on the  
100 behavioural neurobiology of the cuttlefish and their remarkably rapid and apparently  
101 cognitively complex reactions to novel challenges. For instance, cuttlefish can utilise spatial  
102 learning to solve maze tasks based on visual cues (e.g. landmark and e-vector of polarization  
103 light) (Alves et al., 2007, Cartron et al., 2012). Object recognition in cuttlefish (e.g. visual  
104 equivalence, amodal completion and visual interpolation for contour completion) appears to  
105 use strategies close to those used in vertebrates (Zylinski et al., 2012, Lin and Chiao, 2017a,  
106 Lin and Chiao, 2017b). The recent push towards comparisons of advanced cognitive  
107 behaviours (i.e. number sense, episodic-like memory, self-control), has postulated that the  
108 ability of the cuttlefish in solving complex tasks and cognitive reactions approaches that of  
109 young humans (Yang and Chiao, 2016, Schnell et al., 2021a, Schnell et al., 2021b).

110 Our current knowledge of the apparently complex behaviour of cuttlefish is  
111 predominantly derived from a large number of studies on a primarily nocturnal species, *S. officinalis* (Cajal, 1917, Sanders and Young, 1940, Boycott, 1961, Denton and Gilpin-Brown,  
112 1961, Messenger, 1968, Chichery and Chichery, 1987, Nixon and Mangold, 1998, Gaston  
113 and Tublitz, 2004, King et al., 2005, Hanlon et al., 2009, Wild et al., 2015, Oliveira et al.,  
114 2017, Gonzalez-Bellido et al., 2018, Feord et al., 2020, Schnell et al., 2021a, Schnell et al.,  
115 2021b, Osorio et al., 2022). Despite intense interest their cognitive abilities the CNS gross  
116 anatomy, lobe organisation, brain-wide neural networks and the associated functional circuits  
117 is scant compared to both octopuses (Messenger, 1967, Young, 1971, Budelmann and Young,  
118 1985, Plän, 1987, Chung et al., 2022) and loliginid squids (Cajal, 1917, Young, 1974, Young,  
119 1976, Young, 1977, Young, 1979, Messenger, 1979, Wild et al., 2015, Chung et al., 2020).

121 Notably, while some of what we know around biology, ecology and physiology has  
122 also been obtained from the Indo-Pacific species, knowledge of their neuroanatomy is either  
123 sparse (e.g. *S. latimanus*, *S. pharaonis*, *Sepia bandensis* and *Sepiella japonica*) or absent  
124 among distinctively diurnal species such as *S. apama*, the flamboyant cuttlefish (*Metasepia*  
125 *pfefferi*) and the mourning cuttlefish (*Sepia plangon*) (Norman et al., 1999, Hanlon et al.,  
126 2007, Zylinski et al., 2011, Lee et al., 2013, Yang and Chiao, 2016, Liu et al., 2017a, Li et al.,  
127 2018, Schnell et al., 2019, Mezrai et al., 2020, Lu and Chung, 2017, Montague et al., 2022).

128 Recently developed techniques in magnetic resonance imaging (MRI) and histology to  
129 investigate cephalopod brains has revealed numerous novel findings at the morphological  
130 level. In particular, we have linked lobe growth and heterogeneity to ecological niches and  
131 lifestyle (Chung and Marshall, 2017, Liu et al., 2018, Chung et al., 2020, Chung et al., 2022).

132 Diffusion MRI (dMRI) using an ultra-conservative level for tractography acceptance  
133 has accurately delineated several new neural interconnections and networks, and at a level of  
134 detail not possible to see with conventional histology (Chung et al., 2020, Chung et al., 2022).  
135 It is worth noting that the first brain-wide connectome of squid CNS recovered 99.65% of the  
136 previously known neural tracts of loliginids (281 of 282) along with additional dozens of  
137 previously unknown visual-motor related tracts (Chung et al., 2020).

138 Furthermore, in contrast to a regular dorsoventral chiasmata in nocturnal octopuses, a  
139 new form of retinal wiring of the diurnal reef octopus which splits the visual scene into 4  
140 separate zones suggested that this adaptation was linked to their ecology and behaviour  
141 (Chung et al., 2022). These examples highlight the advantage of new MRI-based methods  
142 and how a comparative study of various species, outside the list of the classical model species,  
143 allows evolutionary history to be drawn that may otherwise remain obscured.

144 In this context we asked three questions here: (1) Whether the neural anatomy of *S. officinalis*  
145 may be representative of all or most cuttlefish (over 100 species)? (2) Whether the  
146 cuttlefish brain may have some adaptations in response to their habits and habitats similar to  
147 those found in octopuses (i.e. enlargement and division of their visual centre, structural  
148 foldings and complexity in the learning and memory centre)? (3) Alternatively, given their  
149 free-swimming mode, are their brain adaptations more akin to their apparently closer cousins,  
150 the squid?

151 Understanding the gross neuroanatomy and circuit diagrams of any nervous system is  
152 the necessary first step towards understanding how evolution has shaped both brain structures  
153 and behaviours in cephalopods (Budelmann and Young, 1987, Nixon and Young, 2003,  
154 Williamson and Chrachri, 2004, Chung and Marshall, 2014, Chung and Marshall, 2017, Liu  
155 et al., 2018, Chung et al., 2020, Chung et al., 2022). In order to describe the neuroanatomy of  
156 the cuttlefish species described here, we have used the previous publications of *S. officinalis*  
157 and loliginid squids as a ‘baseline’, along with the few other descriptions for some brain areas  
158 that exist for other cuttlefish species (Cajal, 1917, Boycott, 1961, Young, 1974, Young, 1976,  
159 Young, 1977, Young, 1979, Messenger, 1979, Dubas et al., 1986b, Dubas et al., 1986a,

160 Budelmann and Young, 1987, Wild et al., 2015, Liu et al., 2017a, Gonzalez-Bellido et al.,  
161 2018, Li et al., 2018, Chung et al., 2020, Montague et al., 2022).

162 We also chose a comparative approach, both between cuttlefish species and with squid,  
163 and investigated 2 species of decapodiform cephalopods that represent phylogenetically  
164 distinct groups and that exhibit different life modes, including the reef squid *Sepioteuthis*  
165 *lessoniana* and the diurnal reef cuttlefish, *S. plangon*. In addition to these species described  
166 here, another 9 cuttlefish species (*Metasepia tullbergi*, *Sepia elegans*, *Sepia orbignyana*,  
167 *Sepia omani*, *S. latimanus*, *S. officinalis*, *S. pharaonis*, *S. bandensis*, *S. japonica*) were  
168 selected from published literature (Boycott, 1961, Jereb and Roper, 2005, Wild et al., 2015,  
169 Liu et al., 2017a, Li et al., 2018, Ziegler et al., 2018, Montague et al., 2022) and included for  
170 further analyses where comparative data exists. Observations on the relative enlargement of  
171 brain lobes, and brain folding are included in an extended comparison of species, relative to  
172 ecology and lifestyle as well as phylogenies mostly based on existing morphological and  
173 molecular data.

174

## 175 **Results**

### 176 **Gross anatomy of the diurnal cuttlefish brain**

177 Dissection, contrast-enhanced 16.4T MR images (isotropic resolution 30  $\mu\text{m}$ ) and  
178 resulting 3D reconstruction show that the brain of *S. plangon* is located just under the anterior  
179 projection of the cuttlebone (Figure 1). The central complex (CC) is encased by the cranial  
180 cartilage whereas the two optic lobes (OPLs) are partially covered at the posterior end (Figure  
181 1B). In gross anatomical terms this diurnal cuttlefish possesses a compact brain superficially  
182 similar to those of *S. officinalis* (histology and MRI (3T & 9.4T) (Tompsett, 1939, Boycott,  
183 1961, Wild et al., 2015, Ziegler et al., 2018) and *S. bandensis* (histology and MRI (9.4T))  
184 (Montague et al., 2022) and shares a similar lobe arrangement as the loliginid squids (Young,  
185 1974, Young, 1976, Young, 1977, Young, 1979, Messenger, 1979, Chung et al., 2020),  
186 including 32 lobes (15 of which are bilateral) (Figures 1-2 & Table S1).

187 Notably, the suboesophageal mass of squid is elongated due to the long brachio-pedal  
188 connective to make contact with the brachial lobe further away from the pedal lobe complex  
189 (Figure 2). Additionally, the close to bottom dweller, *S. plangon*, and the water column  
190 dweller, *S. lessoniana*, possess relatively small chemosensory regions (inferior frontal lobe

191 complex (iFLx)), approximately 0.3-0.5% of CNS volume, indicating that chemoreception is  
192 less important than for the entirely benthic octopuses (4-6%) (Maddock and Young, 1987,  
193 Chung et al., 2020, Chung et al., 2022). Several previously unknown neuroanatomical  
194 features, obvious at a gross anatomical level, were identified in *S. plangon*, including distinct  
195 enlargement of the OPL and vertical lobe, and morphological folding of the OPL as described  
196 next (Figures 1-2, Videos S1-2).

197

### 198 **Croissant-shaped optic lobe**

199 All specimens (1 hatchling, 2 juveniles and 3 adults) examined here possess distinct  
200 enlarged OPLs (the percentages of OPLs relative to total CNS volumes range between 77-  
201 82%) which are close to another diurnal cuttlefish *S. latimanus* (ca 82%) (Ziadi-Kunzli et al.,  
202 2019) and those of loliginid squids (e.g. 80% of CNS in *S. lessoniana*; *Sepioteuthis sepioidea*  
203 (79%) and *Loligo forbesi* (77%)) (Maddock and Young, 1987, Chung et al., 2020). This is in  
204 contrast to the moderately-large OPLs (58-74% of CNS) in another 4 cuttlefish species which  
205 are frequently active at low light conditions (Tables 1 & S3).

206 Another unique neuroanatomical feature of *S. plangon* among cuttlefish but one which  
207 it shares with some octopus species (Chung et al., 2022) is an only just described croissant-  
208 shaped OPL. All decapodiform cephalopods examined, as far as we know, have a regular  
209 bean-shaped OPL, including its cuttlefish siblings (e.g. *S. officinalis*, *S. bandensis*, *S.*  
210 *pharaonis*, *S. omani* and *S. japonica*), neritic squid (e.g. *Idiosepius*, *Loligo* and *Sepioteuthis*)  
211 and deep sea squid (e.g. *Abraaliopsis*, *Architeuthis*, *Bathyteuthis*, *Liocranchia* and *Pyroteuthis*)  
212 (Boycott, 1961, Young, 1974, Chung, 2014, Chung and Marshall, 2017, Liu et al., 2017b, Liu  
213 et al., 2017a, Li et al., 2018, Liu et al., 2018, Montague et al., 2022).

214 Given their similar body size, the OPLs of *S. plangon* are significantly larger than those  
215 of the nocturnal *S. bandensis* (ML: 60-70mm) and the reef squid, *S. lessoniana* (ML: ca 110  
216 mm) (Tables 1 & S2-3). The croissant-shaped OPL is present over a broad range of body size  
217 (young juvenile - adult, mantle length: 18-107 mm), less accentuated in the post-hatchling (a  
218 week old) and appears to be associated with a diurnal existence and associating visual tasks  
219 (Figures 2-4). Detailed morphological features are as follows:

220 (i) OPL horns. The dorsal 1/3 of the OPL is divided into two parts, forming two blunt horns  
221 that are closely opposed near the central line of the OPL. With the cuttlefish in a posture that

222 is resting on the substrate or hovering in the water column, the anterior horn receives input  
223 from the posterior visual scene via the posterior vertical slit of its w-shaped pupil. The  
224 posterior horn is opposite to this and receives visual input from the antero-ventral direction,  
225 a zone vital for the ballistic tentacular strike used for prey capture.

226 (ii) OPL sulcal folding. A second modification in *S. plangon* (again one found recently also  
227 in octopus (Chung et al., 2022)) is a curved-shaped sulcus at the lateral side apparently  
228 matched to the central crescent-shaped area of the pupil. The function of these structural  
229 folding is most likely to increase the surface area of the OPL. This is discussed relative to the  
230 gyrification index (GI =1.06) below but in brief appears to correlate with resolution power.

231

## 232 **Vertical lobe**

233 Volumetric estimates show that the dome-shaped vertical lobe of *S. plangon* is  
234 significantly enlarged (4-5.3% of CNS volume) relative to those of the loliginid squids (0.3-  
235 3.2%) and cuttlefish species which are more active in the low light conditions (e.g.  
236 dominantly nocturnal *S. officinalis* (0.3-3.6%), and those living in deeper water (100-400m  
237 depth) such as *S. elegans* (3.2%) and *S. orbignyana* (3.3%)) (Table 1). Additionally, the size  
238 of vertical lobe increases significantly during ontogeny (from 2.4% at hatchling to  
239 approximately 4-5% at adult) (Tables 1 & S3).

240

## 241 **Tractography and connectome of the cuttlefish brain**

242 Using the same imaging procedure and the selection criteria established for the squid  
243 brain (Chung et al., 2020), the averaged connectome of *S. plangon* (3 adults) allows recovery  
244 of all known major inter-lobed tracts described in squid and cuttlefish (n = 388, connectivity  
245 strength of tractography ( $C_s$  the logarithm of numbers of streamlines intersecting a pair of  
246 lobes: 0.48 - 5.76) (Figure 3) (Cajal, 1917, Boycott, 1961, Young, 1974, Young, 1976, Young,  
247 1977, Young, 1979, Messenger, 1979, Budelmann and Young, 1987, Novicki et al., 1990,  
248 Chung et al., 2020). In addition, 181 blank spots ( $C_s = 0$ ) in the averaged connectivity matrix  
249 from tractography are well-matched with the blanks from previous histology, demonstrating  
250 that our current procedure effectively eliminating false positives.

251        Despite the considerable difference in phylogenetic relationship, a comparison of the  
252        MRI-based connectomes confirms a high degree of similarity in the inter-lobed network  
253        between squid and cuttlefish (Figure 3). Notably, the vision-related networks in two inter-  
254        lobed connectomes represent nearly the same pattern, including those connections between  
255        OPL-supra-esophageal mass (squid: 2.44 - 5.08 vs cuttlefish: 3.13 - 5.4) (e.g. OPL linked  
256        with basal lobe complex) and OPL-sub-esophageal mass with the median-high  $C_s$  value  
257        (squid: 0.74 - 4.58 vs cuttlefish: 1.18 - 5.21) (e.g. OPL linked with pedal and magnocellular  
258        lobes). Also, the connectomes within the sub-esophageal mass that are responsible for  
259        locomotion manoeuvre are similar, presumably due to similar modes of locomotion between  
260        the two groups. In addition, a comparison of the  $C_s$  between brachial and inferior frontal  
261        lobes (*S. plangon* (3.77) vs *S. lessoniana* (0.61)) confirms a previous qualitative description  
262        that a strong inter-lobed connection throughout the cerebro-brachial tracts exists in cuttlefish,  
263        *S. officinalis*, whereas fewer stained neurons are seen in squid, *Loligo vulgaris* (Budelmann  
264        and Young, 1987) (Figure 3).

265        A few remarkably strong inter-lobed connections ( $C_s$ : 1.6-2.8) may be identified as  
266        tracks unique to cuttlefish, whereas those in the squid connectome are either absent or with a  
267        much lower  $C_s$  value (<1), including those related to the chromatophore, magnocellular and  
268        pedal lobes (Figure 3D). Considering the main function of these three brain regions, in  
269        control of locomotion and colouration (Boycott, 1961), these previously-unknown  
270        tractographic connections are likely to drive dynamic body pattern changes as well as the two  
271        previously known circuits (OPL-lB-Ch and OPL-PED-lB-Ch) (Messenger, 2001, Gonzalez-  
272        Bellido et al., 2018).

273

## 274 **Phylogenetic analyses**

275        Pagel's  $\lambda$  and phylogenetic generalised least squares (PGLS) analyses were used to  
276        estimate the likelihood that these newly described modifications are phylogenetically linked  
277        (STAR Methods). A strong phylogenetic relationship is linked in the morphological changes  
278        of the optic lobes (Pagel's  $\lambda$  = 0.9999 for all 7 species; test of  $\lambda$  = 1,  $p$  = 1) (Figure 4).  
279        However, we suggest the adaptations seen here, especially those within the OPL in diurnal  
280        reef dwellers are most likely driven by the needs of their life modes. In other animals, it is the  
281        adaptations of the central brains and existing CNS design that are more likely to retain a

282 phylogenetically-flavoured relationship (Yopak et al., 2010, Yopak et al., 2020, Chung et al.,  
283 2022, Wolff et al., 2017, Nixon and Young, 2003).

284

## 285 **Discussion**

286 In common with their major competitors, the fish, coastal cephalopods are successful  
287 and voracious visual predators that live over a broad range of ecological niches. In contrast to  
288 our knowledge of fish neuroanatomical adaptations related to sensory perception, foraging  
289 modes and habitats (Wagner, 2001, Lisney and Collin, 2006, Yopak et al., 2015), establishing  
290 links between behavioural features and neuroanatomical modifications remains in its infancy  
291 for the cephalopods (Ponte et al., 2021). Using MRI-based techniques and conventional  
292 histology, we have started the first detailed comparison of neuroanatomical features and  
293 corresponding MRI-based connectomes between cuttlefish, octopus and squid. This work  
294 focusses on cuttlefish but uses our previous studies on squid and octopus as a comparison,  
295 both to describe differences in basic brain and wiring anatomy and to examine the ecology  
296 and, to an extent, the evolution of the cephalopod brain. It of course stands on the shoulders  
297 of previous work on these brainy invertebrates, notably that of JZ Young and colleagues  
298 (Boycott, 1961, Messenger, 1973, Nixon and Young, 2003) along with a few studies between  
299 that time and now (Chichery and Chanelet, 1976, Chichery and Chanelet, 1978, Chichery and  
300 Chichery, 1987, Dickel et al., 1997, Williamson and Chrachri, 2004, Liu et al., 2017a,  
301 Gonzalez-Bellido et al., 2018).

302 We also present new findings from a comparative approach amongst cuttlefish species  
303 and hope to provide a firm base to challenge the long-standing assumption that  
304 neuroanatomical features of *S. officinalis* are representative of all cuttlefish species. The  
305 neuroanatomical variation we note here infers interspecific variation in visual capabilities, the  
306 importance of vision relative to the less utilised chemosensory system and clear links with  
307 life modes (e.g. diurnal vs nocturnal), ecological factors (e.g. living depth and ambient light  
308 condition) as well as to an extent, phylogeny.

309

## 310 **Unique neuroanatomical features in the mourning cuttlefish, *Sepia plangon***

311 Early reports divided the cuttlefish brain into regions and associated functions based on  
312 electrical stimulation of selected lobes of *S. officinalis* (Boycott, 1961, Chichery and Chanelet,

313 1976, Chichery and Chanelet, 1978, Chichery and Chichery, 1987). However the neuronal  
314 number and circuitry behind these connections has remained largely unknown for now more  
315 than 30 years (Budelmann and Young, 1987). Here MRI-based observations and gross  
316 anatomy have revealed a number of new observations.

317 The tropical diurnal reef cuttlefish, *S. plangon*, apparently possesses an enlarged brain  
318 compared to the other coastal species with a similar given body size. The adult-like hatchling  
319 of *S. plangon* (ML: 8 mm) has an enlarged brain compared to *S. officinalis* (ML: 6.3 mm)  
320 (CNS: 9.26 vs 2.94 mm<sup>3</sup> and OPLs: 7.11 vs 1.97 mm<sup>3</sup>) (Wild et al., 2015). Notably, the  
321 cuttlefish embryo starts to react to visual and chemical cues before hatching (stage 30)  
322 (Darmaillacq et al., 2006, Mezrai et al., 2020). Unlike the eggs of *S. officinalis* which are  
323 darkened by maternal ink resulting in poor visibility of the outside scene, the transparent egg  
324 of *S. plangon* allows the embryo to receive surrounding visual cues and respond accordingly  
325 with flashing chromatophores. This early vision-related demand toward the post-hatching  
326 environment may therefore initiate enlargement of the OPL of *S. plangon* more than that seen  
327 in *S. officinalis* (77% vs 67% of CNS).

328 The CNS of *S. plangon* grows rapidly and particularly the VL and OPLs attain a level  
329 of complexity and volume not seen in previously examined cuttlefish (Table S3). The size  
330 increase of VL during ontogeny results in a 210% relative increase from 2.4% of CNS at  
331 hatchling to approximately 4-5% at adult. Furthermore, growth of the OPL from post-  
332 hatchling to adult is up to 100 fold the volume increase during all life stages, emphasising the  
333 vital role of vision for this diurnal species.

334 Our examination of *S. plangon* shows, like octopus (Chung et al., 2022) two types of  
335 OPLs exist, bean vs croissant shape and that this reflects their phylogenetic relationship, life  
336 modes and habitats (Figure 4). Both nocturnal and deep-water dwelling cuttlefish species  
337 (>200m depth) which encounter dim light condition have a regular bean-shaped OPL (Table  
338 1). In contrast, the diurnal species seem to have the enlarged croissant-shaped OPL, a  
339 modification associated with a more visual existence and first noted in our previous studies  
340 on diurnal octopus species octopus (Chung et al., 2022). By contrast, cuttlefish that live in  
341 low light condition where there is less visual contrast possess smaller OPL than those of the  
342 diurnal species (Ziegler et al., 2018) (Figure 4).

343

#### 344 **Similarity of brain regions between squid and cuttlefish**

345 Squid and cuttlefish predation is remarkably fast and precise. The feeding behaviour  
346 entails a rapid tentacular strike to catch small prey and a ‘punch’ from the arm crown to

347 attack and defend for large objects (Chung and Marshall, 2014, Lu and Chung, 2017, Hanlon  
348 and Messenger, 2018). These ballistic movements are visually-coordinated activities and  
349 include finding a prey item in the distance and, on moving closer, estimating the object size  
350 to guide ballistic strike (Messenger, 1968, Kier and Von Leeuwen, 1997, Chung and Marshall,  
351 2014, Feord et al., 2020). Additionally, assessment of prey quality (acceptation or rejection  
352 for feeding) is based on contact chemoreception via the suckers of the arms and tentacles  
353 (Messenger, 1973, Archdale and Anraku, 2005).

354 The proportion of neural processing investment in chemoreception and vision between  
355 the three coleoid groups (cuttlefish, squid and octopus) is quite variable and this study has  
356 helped uncover new and underline previous observations. All three cephalopod groups  
357 possess optically excellent and often large eyes and all three put considerable investment into  
358 the OPL processing of vision (but see ecological differences discussed in Chung et al. (2022))  
359 (Land, 1981, Sweeney et al., 2007). There is a difference in volume ratio between the two  
360 sensory brain regions, vision (OPLs) versus chemoreception (iFLx), which reaches over 100  
361 fold in cuttlefish (e.g. 101 in *S. officinalis*; 235 in *S. plangon*), > 200 in loliginid squid (e.g.  
362 220 in *S. lessoniana*; 305 in *Loligo forbesi*) compared to a very low value around 10 in the  
363 benthic octopuses, such as *Octopus vulgaris* and *Hapalochlaena fasciata* (Maddock and  
364 Young, 1987, Chung et al., 2020, Chung et al., 2022). The relative value of a given sensory  
365 area clearly shows its level of importance, suggesting again that the water column dwellers  
366 rely more on vision, whereas the more benthic groups favour a combination of vision and  
367 chemoreception.

368 Further to the basic volumetric data, vision-related connectomes highlight that  
369 cuttlefish and squid have adopted similar principles in design in response to visually-  
370 coordinated activities at a very fine scale (Figures 2-3). These two groups possess similar  
371 network matrices within the vision to higher motor brain regions (e.g. basal lobe complex)  
372 (Figure 3).

373 Again vision related, the multilayered structure in all basal lobes show tractographic  
374 projections from the upper layers of the basal lobes that connect only with the upper level of  
375 the optic lobe, whereas the projections from the lower levels of the basal lobes shift toward  
376 lower levels of the optic lobe accordingly (Chung et al., 2020) (Video S3). This multi-layered  
377 network arrangement likely retains retinotopic spatial information from the outside world  
378 through to the motor command units in the BLs (Young, 1977, Chung et al., 2020).

379 Finally, this direct connection from visual input in to motor action out is underlined by  
380 the new finding that the basal lobe complex possesses interweaving circuits with the sub-

381 esophageal mass. This suggests a relay station exists, mediating motor control such as arm  
382 movements (brachial lobe), tentacular strike and eye movements (pedal lobes) and funnel and  
383 fin movements (magnocellular, fin and palliovisceral lobes) (Boycott, 1961, Young, 1976,  
384 Chichery and Chichery, 1987, Budelmann and Young, 1987, Chung et al., 2020).

385

### 386 **Cuttlefish-unique neural network features related to chemoreception, colouration and 387 camouflage?**

388 While there is a degree of similarity in inter-lobed connectivity between cuttlefish and  
389 squid brains, there are also other tractographic, network and gross anatomical features unique  
390 to cuttlefish. These again appear largely driven by ecology and behavioural habits. In brief  
391 they are the network between iFLx and brachial lobe (chemosensory related circuits) and  
392 those amongst chromatophore, magnocellular and pedal lobes (colouration related circuits)  
393 (Figure 3). Each of these cuttlefish-unique features is now described in more detail based  
394 around suggested function.

395

### 396 **Cheosensory-learning circuits**

397 At gross anatomic levels, the volumetric ratio between iFLx and OPLs in squids is  
398 smaller than in cuttlefishes in both temperate (e.g. *L. vulgaris* vs *S. officinalis*) and tropical  
399 (e.g. *S. lessoniana* vs *S. plangon*) species (Maddock and Young, 1987, Chung et al., 2020). In  
400 addition, the increasing complexity of neural network between brachial lobe and iFLx in  
401 cuttlefish indicate that cuttlefish may favour chemosensory cues in daily tasks and more so  
402 than squid (Figures 2-3). In the behavioural context, bait coated with additional chemicals or  
403 biological extract (e.g. amino acids, quinine or cephalopod ink), may be accepted or rejected  
404 by touching the bait using arms/tentacles in the cuttlefish, *Sepia esculenta* (Archdale and  
405 Anraku, 2005). A similar bait handling behaviour has been found in the other 2 cuttlefish, *S.*  
406 *plangon* and *S. latimanus*, during feeding training in captivity. Using the same method rarely  
407 triggered feeding acceptance by squid such as *S. lessoniana* that appear to need movement  
408 cues to trigger bait capture (personal observation). This indicates that cuttlefish maintains  
409 good contact chemosensory capabilities, somewhere between octopus and squid, which could  
410 be helpful to shape prey preference and tune foraging strategies.

411

### 412 **Additional colouration related circuits in cuttlefish**

413 Numerous novel projectomes related the cuttlefish chromatophore lobe ( $C_s > 1.5$ ) are  
414 identified in the matrix (Figure 3D). Although the function of this network remains unclear,

415 two possible explanations are proposed as follows: (1) Ontogenetic differences. (2)  
416 Additional circuits related to body patterns.

417

418 (1) Ontogenetic differences

419 The cephalopod brain grows continuously over a long period time during its limited 1-2  
420 year life span. This is accompanied by an increasing complexity of behaviours (Messenger,  
421 1973, Nixon and Young, 2003, Chung et al., 2020, Chung et al., 2022). For instance, the  
422 hatching of *S. plangon* only shows two simple body patterns (uniform darkening and blanching)  
423 in contrast to the diverse colouration displays during courtship and sophisticated camouflage  
424 and warning patterns (Alejandra et al., 2020). Considering the current squid connectome  
425 based on 5 juveniles (ML: 40-113 mm) along with other supporting neural tracing data that  
426 also favoured smaller brains (mainly juveniles) (Young, 1976, Budelmann and Young, 1987,  
427 Novicki et al., 1990, Chung et al., 2020), a comparison between the two connectomes (adult  
428 cuttlefish vs juvenile squid) could therefore miss some connections which appear only at the  
429 adult stage.

430

431 (2) Additional circuits related to cuttlefish body patterns

432 Decapodiform cephalopods show several forms of courtship display which visually  
433 attract mates and coordinates copulation activities (Brown et al., 2012, Lin et al., 2017,  
434 Hanlon and Messenger, 2018, Alejandra et al., 2020). Cuttlefish courtship display has been  
435 well documented in a few species, including *S. latimanus*, *S. officinalis* and *S. plangon*. These  
436 displays often use a combination of chromatic, textural and postural components (Hanlon and  
437 Messenger, 2018, Alejandra et al., 2020). For instance, *S. plangon* uses 34 chromatic  
438 components combined with 3 textural and 14 postural components for dynamic courtship  
439 displays (11 patterns used by female; 18 by male) (Alejandra et al., 2020). In contrast, squid  
440 mainly relies on chromatic components alone such as *S. lessoniana* assembling 27 chromatic  
441 components during reproductive interactions (7 patterns used by female; 12 by male) (Lin et  
442 al., 2017). It should be remembered that both groups are most likely colour blind, seeing only  
443 the luminance and pattern component of such displays (Marshall and Messenger, 1996,  
444 Chung and Marshall, 2016).

445 The complexity of camouflage tricks between cuttlefish and squid is also substantial.  
446 Cuttlefish camouflage contains a combination of cryptic colouration, skin texture and arm  
447 posture to conceal itself into the 3D characters of the surrounding scene (e.g. algae, rubbles,

448 coral) (How et al., 2017, Gonzalez-Bellido et al., 2018, Hanlon and Messenger, 2018). By  
449 contrast, the squid mainly relies on colour changes on body surface to mimic the 2D  
450 background such as manipulating colours to match with substrate while reaching close to  
451 floor and switching to countershading while hovering in water column (e.g. *S. lessoniana*)  
452 (Lu and Chung, 2017, How et al., 2017, Nakajima et al., 2022). Both chromatic and hydrostat  
453 systems are regularly used in the formation of cuttlefish body patterns (Gonzalez-Bellido et  
454 al., 2018, Alejandra et al., 2020, Osorio et al., 2022), and one additional set of neural  
455 components to coordinate those apparently more complex body patterns compared to a  
456 relatively simple system used for the squid chromatic-based patterns is revealed here (Figure  
457 3). The detailed function will need further tests to clarify what these additional circuits  
458 achieve relative to neural and behavioural dynamics and how the cuttlefish nervous system  
459 dispatches signals via different pathways to govern skin patterns (Laan et al., 2014, Reiter et  
460 al., 2018, Osorio et al., 2022).

461

## 462 [Elongated CNS layout linked to the streamline body shape](#)

463 3D reconstruction of the coastal decapodiform brain clearly showed that distinct CNS  
464 elongation appears in the myopsid squid and not in cuttlefish (Figure 2). Firstly, with the  
465 absence of a floatation apparatus, the cuttlebone, to offset gravity, squid rely on constant  
466 swimming to maintain buoyancy and direction, resulting in a daily energy cost much higher  
467 than that of the neutral buoyant cuttlefish (O'Dor, 2002). This means that a long, streamlined  
468 body shape that minimises energy consumption is desirable for squid (O'Dor and Webber,  
469 1986). In turn this has resulted in a stretched squid brain, to fit within this body shape and  
470 prevent its brachial and optic lobes bulging outward, causing higher drag. A similar  
471 observation of a further elongated CNS layout was briefly described in the oceanic oegopsid  
472 squid (neon flying squid) by Nixon and Young (2003)), again suggesting that development of  
473 the streamline body shape of squid might be therefore co-evolved with its elongated CNS.

474

475

476

477

478

479 **Materials and Methods**

480 **Sample collection and preparation**

481 All collections were conducted under a Great Barrier Reef Marine Park Permit  
482 (G17/38160.1) and Queensland General Fisheries Permit (180731). The mourning cuttlefish,  
483 *Sepia plangon*, and oval squid, *Sepioteuthis lessoniana*, were collected using a seine net  
484 (water depth 1-3m) close to Moreton Bay Research Station, Stradbroke Island, Queensland,  
485 Australia. The maintenance and experimental protocol used here were covered by animal  
486 ethics permit (QBI/236/13/ARC/US AIRFORCE & QBI/304/16). Total 44 cuttlefish and 5  
487 squid were collected for this neuroanatomical study in 2017-2021.

488 Animals were anaesthetised in cool seawater (15°C) mixed with 2% MgCl<sub>2</sub> (Chem-  
489 Supply, Australia) and sacrificed by an overdose of MgCl<sub>2</sub> prior to fixation. The small  
490 specimens (hatchlings and early juvenile) were soaked into 4% PFA-PBS fixative at 4°C for  
491 48 h and then transferred to 0.1% PFA-PBS fixative for storage at 4 °C until further  
492 dissection.

493 Three adult cuttlefish specimens for MR imaging were fixed using the transcardial  
494 perfusion protocol developed by Chung et al. (2020). In brief, the transcardial perfusion  
495 protocol is using 4% paraformaldehyde (PFA) (EM grade, Electron Microscopy Sciences,  
496 Hatfield, USA) mixed with 0.1 M PBS with the rate of perfusion set to 2.5 ml per minute.  
497 The perfusion proceeded until 0.2 ml fixative per gram of specimen was used. Subsequently  
498 the muscle, skin and connective tissues around the brain were removed and the specimen was  
499 soaked in 4% PFA-PBS fixative for overnight to reduce morphological deformation of the  
500 brain.

501

502 **Image stacking of the isolated brain-eyes**

503 The isolated brain and eyes were imaged with the focus stacking method using a digital  
504 camera (Canon 5D4 camera with Canon MPE 65mm Macro lens, Canon, Japan) mounted on  
505 the electronically-controlled focusing rack (Castel-Micro focusing rack, Novoflex, Germany).  
506 A sequence of close-up images was captured from the dorsal end of brain to the ventral end  
507 using 0.1 mm step for small samples or 0.25 mm step for large samples. Focus stacking (20-  
508 80 images) was processed using the software Helicon Focus Pro (version 7.6.4, Helicon Soft  
509 Ltd. Ukraine), rendering an image with a greater depth of field.

510 **MRI procedure**

511 Intact brain and eyeballs were isolated and repeatedly rinsed with 0.1 M PBS to  
512 minimise fixative residue. The isolated brain and eyes were then soaked into 0.1 M PBS  
513 containing magnetic resonance imaging (MRI) contrast agent, 0.2% ionic Gd-DTPA  
514 (Magnevist) (Bayer, Leverkusen, Germany), for 24-48 hours to enhance image contrast prior  
515 to MR imaging (Chung et al., 2020, Chung et al., 2022). Six contrast-enhanced cuttlefish  
516 brains were imaged following the protocol developed by Chung et al. (2020). The contrast-  
517 enhanced specimen was placed into a fomblin-filled (Fomblin oil, Y06/6 grade, Solvay, USA)  
518 container to prevent dehydration and then vacuumed for 3 minutes to remove air bubbles  
519 trapped inside oesophagus or brain lobes. The container was then placed in a custom-built 20  
520 mm diameter surface acoustic wave coil or 10 mm diameter quadrature coil (M2M Imaging,  
521 Brisbane, Australia). Both high resolution MR structural images and high angular resolution  
522 diffusion images (HARDI) were acquired using a 16.4 Tesla (700 MHz) vertical wide-bore  
523 microimaging system (interfaced to an AVANCE I spectrometer running imaging software  
524 Paravision 6.0.1 (Bruker Biospin, Karlsruhe, Germany) in the Centre for Advanced Imaging  
525 at the University of Queensland. Imaging was performed at a room temperature (22 °C) using  
526 a circulating water-cooling system.

527 Three dimensional (3D) high resolution structural images were acquired using fast low  
528 angle shot (FLASH) with the following parameters based on Chung and Marshall (2017):  
529 echo time (TE) / repetition time (TR) = 12/40 ms, average = 4, flip angle (FA) = 30°, field of  
530 view (FOV) =  $7.5 \times 6.4 \times 6$  mm to  $21 \times 13 \times 13$  mm for different individuals, 30  $\mu\text{m}$   
531 isotropic resolution. Total acquisition time for one brain was 1 h (hatchling) to 8.3 h (the  
532 largest brain).

533 After FLASH imaging, 3D high angular resolution diffusion-weighted imaging  
534 (HARDI) was acquired with the following parameters: TR = 300 ms, TE = 22 ms, 30  
535 direction diffusion encoding with b-value = 3000 s/mm<sup>2</sup>, two b0 images acquired without  
536 diffusion weighting and 80  $\mu\text{m}$  isotropic resolution with 1.5 partial Fourier acceleration  
537 acquisition in the phase dimensions (Chung et al., 2020). Total acquisition time for one brain  
538 was 16.5-35.5 h.

539 **Estimates of lobe volume**

540 Identification of the cuttlefish brain lobes was based on the published anatomical  
541 studies of cuttlefish and loliginid squids as an initial aid in determining the boundaries

542 between tissue. 47 lobes previously defined by (Young, 1974, Young, 1976, Young, 1977,  
543 Young, 1979, Messenger, 1979, Chung et al., 2020, Boycott, 1961) were identified from the  
544 MRI data. The parcellation of the selected lobes and brains was then manually segmented  
545 using MRtrix3 (version 3.0.2, open-source software, <http://www.mrtrix.org/>) (Tournier et al.,  
546 2019) and then estimates of volume of the selected lobes and an entire brain were calculated  
547 using ITK-SNAP (version 3.6.0, open-source software, <http://www.itksnap.org/>) (Yushkevich  
548 et al., 2006). Considering variations of volume estimates of cephalopod brain which are  
549 strongly affected by the size and age of the individuals, the volumes of the lobes were  
550 expressed as percentages of the total CNS volume to circumvent this issue as suggested in  
551 previous studies (Maddock and Young, 1987, Chung et al., 2020, Chung et al., 2022).

552

### 553 **Construction of structural neural connectivity matrix**

554 Our previous work demonstrated that the high resolution HARDI combined with  
555 conservative selection criteria enabled to accurately reveal the major neural tracks in the  
556 squid brain and octopus optic nerve tracks (Chung et al., 2020, Chung et al., 2022). Adapting  
557 the same procedure to construct the brain-wide tractography of cuttlefish brain, the 47 lobes,  
558 regions of interest (ROIs) were used to construct tractography. Probabilistic fibre tracking  
559 was then performed using second order integration over the fibre orientation distribution  
560 (FOD) algorithm and the tracts were generated independently for each ROI (10 streamlines  
561 per voxel) with an optimized FOD amplitude cut-off value of 0.175 to generate biologically  
562 realistic tractography in cephalopod neural tissue at mesoscale. The brain-wide cuttlefish  
563 neural connectivity matrix where the connections and the corresponding connectivity strength  
564 ( $C_s$ ) were mapped to the relevant cuttlefish brain lobes for each individual. The averaged  
565 pairwise  $C_s$  were also calculated and plotted in the matrices for further analysis with the  
566 previously-published squid matrix (Chung et al., 2020).

567

### 568 **Contour-based measurement of gyration index (GI)**

569 The degree of folding of the optic lobe was measured using the contour-based method  
570 (Chung et al., 2022). We measured the GI by comparing the lengths of complete and outer  
571 contours of the selected brain lobes in a serial horizontal MR slices for the OPLs along with  
572 the dorso-ventral axis using Fiji (version 1.53c, open-source software, <https://imagej.net/>)

573 (Schindelin et al., 2012). The mean GI of the defined entire lobe is the ratio between the sum  
574 of the total outer contour and the sum of the superficially exposed surface contours.

575

## 576 **Phylogenetic analyses**

577 In order to understand whether the phylogenetic relationship or the life mode affect the  
578 modification of octopodiform's brain, the phylogenetic generalised least squares (PGLS) test  
579 was used to investigate the impact of several predictor variables (life modes, light conditions,  
580 and visual tasks) on the modification of neuroanatomical structure while controlling for  
581 potential phylogenetic signals in the responses (Mundry, 2014). Determination of the selected  
582 octopus phylogenetic relationships was based on the published complete mitochondrial DNA  
583 sequence which were available from GenBank. Alignments of sequence were constructed  
584 using the multiple sequence alignment (MUSCLE) method with MEGA X (molecular  
585 evolutionary genetics analysis program version 10.2.5) (Kumar et al., 2018). *Sepioteuthis*  
586 *lessoniana* was used as the outgroup. The phylogenetic tree of these selected species was  
587 generated by the Maximum-Likelihood method and the bootstrap confidence values (1000  
588 replicates) were calculated with MEGA X (Kumar et al., 2018). The phylogenetic signal was  
589 estimated with Pagel's  $\lambda$  using the package the CAPER v1.0.1 as implemented in the RStudio  
590 v1.4.1103. The relationship between the changes of brain anatomy and environmental  
591 characters (Table S3) was determined using the phylogenetic generalised least squares (PGLS)  
592 method with the CAPER package in RStudio.

593

## 594 **Acknowledgements**

595 This work is supported by the Australian Research Council (ARC) (Australian Laureate  
596 Fellowship (FL140100197) to N.J.M.), (Discovery Project (DP200101930) to N.J.M.) and  
597 the Office of Naval Research Global (ONR Global) (N62909-18-1-2134 to N.J.M.) The  
598 16.4T is supported by the Queensland State Government through the Queensland NMR  
599 Network, and the Australian Government through National Collaborative Research  
600 Infrastructure Strategy (NCRIS) and the National Imaging Facility. We thank the staff of the  
601 Moreton Bay Research Station for logistical support. We also acknowledge the  
602 Quandamooka people as the Traditional Owners and their custodianship of the lands on  
603 which Moreton Bay Research Station operate. We pay our respects to their ancestors and

604 their descendants, who continue cultural and spiritual connections to Country and recognise  
605 their valuable contributions to Australian and global society.

606

607 **Author contributions**

608 Conceptualization, W.-S.C. and A.L.G.; methodology, A.L.G. N.D.K. and W.-S.C.; funding  
609 acquisition and supervision, N.J.M.; validation and visualization, W.-S.C. N.D.K. and N.J.M.;  
610 the first draft of manuscript, W.-S.C.; all authors contributed to data analysis, interpretation  
611 and revision of the manuscript.

612

613 **Declaration of Interests**

614 The authors declare no competing interests.

615

616 **References**

617 ALEJANDRA, L. G., CHUNG, W.-S. & MARSHALL, N. J. 2020. Dynamic courtship signals and mate  
618 preferences in *Sepia plangon*. *Front Physiol*, 11, 845.

619 ALLCOCK, A. L., LINDGREN, A. & STRUGNELL, J. M. 2014. The contribution of molecular data to our  
620 understanding of cephalopod evolution and systematics: a review. *J Nat Hist*, 49, 1373-1421.

621 ALVES, C., CHICHERY, R., BOAL, J. G. & DICKEL, L. 2007. Orientation in the cuttlefish *Sepia officinalis*:  
622 response versus place learning. *Anim Cogn*, 10, 29-36.

623 ARCHDALE, M. V. & ANRAKU, K. 2005. Feeding behavior in scyphozoa, crustacea and cephalopoda.  
624 *Chem Senses*, 30 Suppl 1, i303-4.

625 BOYCOTT, B. B. 1953. The chromatophore system of cephalopods. *Proceedings of the Linnean  
626 Society of London*, 164, 235-240.

627 BOYCOTT, B. B. 1961. The functional organization of the brain of the cuttlefish *Sepia officinalis*. *Proc  
628 Biol Sci*, 153, 503-534.

629 BOYCOTT, B. B. & YOUNG, J. Z. 1950. The comparative study of learning. *Physiological mechanisms in  
630 animal behaviour*. Cambridge: The University Press.

631 BROWN, C., GARWOOD, M. P. & WILLIAMSON, J. E. 2012. It pays to cheat: tactical deception in a  
632 cephalopod social signalling system. *Biol Lett*, 8, 729-32.

633 BUDELMANN, B. U. & YOUNG, J. Z. 1985. Central pathways of the nerves of the arms and mantle of  
634 *Octopus*. *Philos T Roy Soc B*, 310, 109-122.

635 BUDELMANN, B. U. & YOUNG, J. Z. 1987. Brain pathways of the brachial nerves of *Sepia* and *Loligo*.  
636 *Philos Trans R Soc Lond B Biol Sci*, 315, 345-352.

637 CAJAL, S. R. 1917. *Contribucion al conocimiento de la retina y centros opticos de los cefalopodos.*  
638 *Tarabajos del laboratorio de investigaciones biologicas de la universidad de Madrid* Madrid.

639 CARTRON, L., DARMAILACQ, A. S., JOZET-ALVES, C., SHASHAR, N. & DICKEL, L. 2012. Cuttlefish rely  
640 on both polarized light and landmarks for orientation. *Anim Cogn*, 15, 591-6.

641 CHIAO, C. C. & HANLON, R. 2001. Cuttlefish camouflage: visual perception of size, contrast and  
642 number of white squares on artificial checkerboard substrata initiates disruptive colouration.  
643 *J Exp Biol*, 204, 2119-2125.

644 CHICHERY, M. P. & CHICHERY, R. 1987. The anterior basal lobe and control of prey-capture in the  
645 cuttlefish (*Sepia officinalis*). *Physiol Behav*, 40, 329-36.

646 CHICHERY, R. & CHANELET, J. 1976. Motor and behavioural responses obtained by stimulation with  
647 chronic electrodes of the optic lobe of *Sepia officinalis*. *Brain Research*, 105, 525-532.

648 CHICHERY, R. & CHANELET, J. 1978. Motor responses obtained by stimulation of the peduncle lobe  
649 of *Sepia officinalis* in chronic experiments. *Brain Research*, 150, 188-193.

650 CHUNG, W.-S. 2014. *Comparisons of visual capabilities in modern cephalopods from shallow water to*  
651 *deep sea*. Phd, The University of Queensland.

652 CHUNG, W.-S., KURNIAWAN, N. D. & MARSHALL, N. J. 2020. Toward an MRI-based mesoscale  
653 connectome of the squid brain. *iScience*, 23, 100816.

654 CHUNG, W.-S. & MARSHALL, N. J. 2014. Range-finding in squid using retinal deformation and image  
655 blur. *Curr Biol*, 24, R64-R65.

656 CHUNG, W.-S. & MARSHALL, N. J. 2016. Comparative visual ecology of cephalopods from different  
657 habitats. *Proc Biol Sci*, 283, 20161346.

658 CHUNG, W.-S. & MARSHALL, N. J. 2017. Complex visual adaptations in squid for specific tasks in  
659 different environments. *Front Physiol*, 8, 105.

660 CHUNG, W. S., KURNIAWAN, N. D. & MARSHALL, N. J. 2022. Comparative brain structure and visual  
661 processing in octopus from different habitats. *Curr Biol*, 32, 97-110 e4.

662 DARMAILLACQ, A. S., CHICHERY, R. & DICKE, L. 2006. Food imprinting, new evidence from the  
663 cuttlefish *Sepia officinalis*. *Biol Lett*, 2, 345-347.

664 DENTON, E. J. & GILPIN-BROWN, J. B. 1961. The effect of light on the buoyancy of the cuttlefish. *J*  
665 *Mar Biol Assoc UK*, 41, 343-350.

666 DICKE, L., CHICHERY, M. P. & CHICHERY, R. 1997. Postembryonic maturation of the vertical lobe  
667 complex and early development of predatory behavior in the cuttlefish (*Sepia officinalis*).  
668 *Neurobiol Learn Mem* 67, 150-160.

669 DRERUP, C. & COOKE, G. M. 2021. Shoaling behaviour in the European cuttlefish *Sepia officinalis*.  
670 *Ethology*, 127, 1101-1108.

671 DUBAS, F., HANLON, R. T., FERGUSON, G. P. & PINSKER, H. M. 1986a. Localization and stimulation of  
672 chromatophore motoneurons in the brain of the squid, *Lolliguncula brevis*. *J Exp Biol*, 121, 1-  
673 25.

674 DUBAS, F., LEONARD, R. B. & HANLON, R. T. 1986b. Chromatophore motoneurons in the brain of the  
675 squid, *Lolliguncula brevis* - an HRP study. *Brain Res*, 374, 21-29.

676 FEORD, R. C., SUMNER, M. E., PUSDEKAR, S., KALRA, L., GONZALEZ-BELLIDO, P. T. & WARDILL, T. J.  
677 2020. Cuttlefish use stereopsis to strike at prey. *Sci Adv*, 6, eaay6036.

678 GASTON, M. R. & TUBLITZ, N. J. 2004. Peripheral innervation patterns and central distribution of fin  
679 chromatophore motoneurons in the cuttlefish *Sepia officinalis*. *J Exp Biol*, 207, 3089-98.

680 GONZALEZ-BELLIDO, P. T., SCAROS, A. T., HANLON, R. T. & WARDILL, T. J. 2018. Neural Control of  
681 Dynamic 3-Dimensional Skin Papillae for Cuttlefish Camouflage. *iScience*, 1, 24-34.

682 HANLON, R. T., CHIAO, C. C., MÄTHGER, L. M., BARBOSA, A., BURESCH, K. C. & CHUBB, C. 2009.  
683 Cephalopod dynamic camouflage: bridging the continuum between background matching  
684 and disruptive coloration. *Philos Trans R Soc Lond B Biol Sci*, 364, 429-437.

685 HANLON, R. T. & MESSENGER, J. B. 2018. *Cephalopod Behaviour*, Cambridge, Cambridge University  
686 Press.

687 HANLON, R. T., NAUD, M.-J., SHAW, P. W. & HAVENHAND, J. N. 2005. Transient sexual mimicry leads  
688 to fertilization. *Nature*, 433, 212-212.

689 HANLON, R. T., NAUD, M. J., FORSYTHE, J. W., HALL, K., WATSON, A. C. & MCKECHNIE, J. 2007.  
690 Adaptable night camouflage by cuttlefish. *Am Nat*, 169, 543-551.

691 HOW, M. J., NORMAN, M. D., FINN, J., CHUNG, W.-S. & MARSHALL, N. J. 2017. Dynamic skin patterns  
692 in cephalopods. *Front Physiol*, 8, 393.

693 JEREB, P., ROPER, C. F., NORMAN, M. D. & FINN, J. 2014. Cephalopods of the world. An annotated  
694 and illustrated catalogue of cephalopod species known to date. Volume 3 Octopods and

695 vampire squids. *FAO species catalogue for fishery purposes*. Roma: Food and Agriculture  
696 Organization of the United Nations.

697 JEREB, P. & ROPER, C. F. E. 2005. Cephalopods of the world. An annotated and illustrated catalogue  
698 of cephalopod species known to date. Volume 1. Chambered nautiluses and sepioids. *FAO  
699 species catalogue for fishery purposes*. Rome: Food and Agriculture Organization of the  
700 United Nations.

701 JEREB, P. & ROPER, C. F. E. 2010. Cephalopods of the world. An annotated and illustrated catalogue  
702 of cephalopod species known to date. Volume 2 Myopsid and oegopsid squids. *FAO species  
703 catalogue for fishery purposes*. Roma: Food and Agriculture Organization of the United  
704 Nations.

705 JOZET-ALVES, C., BERTIN, M. & CLAYTON, N. S. 2013. Evidence of episodic-like memory in cuttlefish.  
706 *Curr Biol*, 23, R1033-5.

707 KIER, W. & VON LEEUWEN, J. 1997. A kinematic analysis of tentacle extension in the squid *Loligo  
708 pealei*. *J Exp Biol*, 200, 41-53.

709 KING, A. J., HENDERSON, S. M., SCHMIDT, M. H., COLE, A. G. & ADAMO, S. A. 2005. Using ultrasound  
710 to understand vascular and mantle contributions to venous return in the cephalopod *Sepia  
711 officinalis* L. *J Exp Biol*, 208, 2071-2082.

712 KUMAR, S., STECHER, G., LI, M., KNYAZ, C. & TAMURA, K. 2018. MEGA X: Molecular Evolutionary  
713 Genetics Analysis across Computing Platforms. *Mol Biol Evol*, 35, 1547-1549.

714 LAAN, A., GUTNICK, T., KUBA, M. J. & LAURENT, G. 2014. Behavioral analysis of cuttlefish traveling  
715 waves and its implications for neural control. *Curr Biol*, 24, 1737-1742.

716 LAND, M. F. 1981. Optics and vision in invertebrates. In: AUTRUM, H. (ed.) *Handbook of Sensory  
717 Physiology*. Berlin: Springer.

718 LEE, Y. H., CHANG, Y. C., YAN, H. Y. & CHIAO, C. C. 2013. Early visual experience of background  
719 contrast affects the expression of NMDA-like glutamate receptors in the optic lobe of  
720 cuttlefish, *Sepia pharaonis*. *J Exp Mar Biol Ecol*, 447, 86-92.

721 LI, Y., CAO, Z., LI, H., LIU, H., LU, Z. & CHI, C. 2018. Identification, characterization, and expression  
722 analysis of a FMRFamide-like peptide gene in the common Chinese cuttlefish (*Sepiella  
723 japonica*). *Molecules*, 23, 742.

724 LIN, C.-Y., TSAI, Y.-C. & CHIAO, C.-C. 2017. Quantitative analysis of dynamic body patterning reveals  
725 the grammar of visual signals during the reproductive behavior of the oval squid *Sepioteuthis  
726 lessoniana*. *Front Ecol Evol*, 5, 30.

727 LIN, I.-R. & CHIAO, C.-C. 2017a. Visual equivalence and amodal completion in cuttlefish. *Front Physiol*,  
728 8, 40.

729 LIN, I. R. & CHIAO, C. C. 2017b. Visual equivalence and amodal completion in cuttlefish. *Front Physiol*,  
730 8, 40.

731 LISNEY, T. J. & COLLIN, S. P. 2006. Brain morphology in large pelagic fishes: a comparison between  
732 sharks and teleosts. *J Fish Biol*, 68, 532-554.

733 LIU, Y.-C., CHUNG, W.-S., YU, C.-C., HSU, S.-T., CHAN, F.-L., LIU, T.-H., SU, C.-H., HWU, Y., MARSHALL,  
734 N. J. & CHIAO, C. C. 2018. Morphological changes of the optic lobe from late embryonic to  
735 adult stages in oval squids *Sepioteuthis lessoniana*. *J Morphol*, 279, 75-85.

736 LIU, Y. C., LIU, T. H., SU, C. H. & CHIAO, C. C. 2017a. Neural organization of the optic lobe changes  
737 steadily from late embryonic stage to adulthood in cuttlefish *Sepia pharaonis*. *Front Physiol*,  
738 8, 538.

739 LIU, Y. C., LIU, T. H., YU, C. C., SU, C. H. & CHIAO, C. C. 2017b. Mismatch between the eye and the  
740 optic lobe in the giant squid. *R Soc Open Sci*, 4, 170289.

741 LU, C.-C. & CHUNG, W.-S. 2017. *Guide of the Cephalopods of Taiwan*, Taichung, National Museum of  
742 Natural Science.

743 MADDOCK, L. & YOUNG, J. Z. 1987. Quantitative differences among the brains of cephalopods. *J Zool*,  
744 212, 739-767.

745 MARSHALL, N. J. & MESSENGER, J. B. 1996. Colour-blind camouflage. *Nature*, 382, 408-409.

746 MESSENGER, J. B. 1967. The peduncle lobe: a visuo-motor centre in octopus. *Proc Biol Sci*, 167, 225-  
747 251.

748 MESSENGER, J. B. 1968. The visual attack of the cuttlefish, *Sepia officinalis*. *Anim Behav*, 16, 342-357.

749 MESSENGER, J. B. 1973. Learning performance and brain structure: a study in development. *Brain*  
750 *Res*, 58, 519-523.

751 MESSENGER, J. B. 1979. The nervous system of *Loligo*. IV. Peduncle and olfactory lobes. *Philos Trans*  
752 *R Soc Lond B Biol Sci*, 285, 275-309.

753 MESSENGER, J. B. 2001. Cephalopod chromatophores: neurobiology and natural history. *Biol Rev*  
754 *Camb Philos Soc*, 76, 473-528.

755 MEZRAI, N., ARDUINI, L., DICKEL, L., CHIAO, C. C. & DARMAILLACQ, A. S. 2020. Awareness of danger  
756 inside the egg: Evidence of innate and learned predator recognition in cuttlefish embryos.  
757 *Learn Behav*, 48, 401-410.

758 MONTAGUE, T. G., RIETH, I. J., GJERSWOLD-SELLECK, S., GARCIA-ROSALES, D., ANEJA, S., ELKIS, D.,  
759 ZHU, N., KENTIS, S., RUBINO, F. A., NEMES, A., WANG, K., HAMMOND, L. A., EMILIANO, R.,  
760 OBER, R. A., GUO, J. & AXEL, R. 2022. A brain atlas of the camouflaging dwarf cuttlefish,  
761 *Sepia bandensis*. *bioRxiv*, 2022.01.23.477393.

762 MUNDRY, R. 2014. Statistical issues and assumptions of phylogenetic generalized least squares. In:  
763 GARAMSZEGI, Z. L. (ed.) *Modern Phylogenetic Comparative Methods and Their Application in*  
764 *Evolutionary Biology: Concepts and Practice*. Berlin, Heidelberg: Springer Berlin Heidelberg.

765 NAKAJIMA, R., LAJBNER, Z., KUBA, M. J., GUTNICK, T., IGLESIAS, T. L., ASADA, K., NISHIBAYASHI, T. &  
766 MILLER, J. 2022. Squid adjust their body color according to substrate. *Sci Rep*, 12, 5227.

767 NIXON, M. & MANGOLD, K. 1998. The early life of *Sepia officinalis*, and the contrast with that of  
768 *Octopus vulgaris* (Cephalopoda). *J Zool*, 245, 407-421.

769 NIXON, M. & YOUNG, J. Z. 2003. *The Brains and Lives of Cephalopods*, Oxford, Oxford University  
770 Press.

771 NORMAN, M. D., FINN, J. & TREGENZA, T. 1999. Female impersonation as an alternative  
772 reproductive strategy in giant cuttlefish. *Proc Biol Sci*, 266, 1347-1349.

773 NOVICKI, A., BUDELMANN, B. U. & HANLON, R. T. 1990. Brain pathways of the chromatophore  
774 system in the squid *Lolliguncula brevis*. *Brain Res*, 519, 315-323.

775 O'DOR, R. 2002. Telemetered cephalopod energetics: Swimming, soaring, and blimping. *Integr Comp*  
776 *Biol*, 42, 1065-1070.

777 O'DOR, R. K. & WEBBER, D. M. 1986. The constraints on cephalopods: why squid aren't fish. *Can J*  
778 *Zool*, 64, 1591-1605.

779 OLIVEIRA, C. C. V., GRANO-MALDONADO, M. I., GONCALVES, R. A., FRIAS, P. A. & SYKES, A. V. 2017.  
780 Preliminary results on the daily and seasonal rhythms of cuttlefish *Sepia officinalis* (Linnaeus,  
781 1758) locomotor activity in captivity. *Fishes*, 2, 9.

782 OSORIO, D., MENAGER, F., TYLER, C. W. & DARMAILLACQ, A. S. 2022. Multi-level control of adaptive  
783 camouflage by European cuttlefish. *Curr Biol*, 32.

784 PLÄN, T. 1987. *Functional neuroanatomy of sensory motor lobes of the brain of Octopus vulgaris* Phd,  
785 University of Regensburg.

786 PONTE, G., TAITE, M., BORRELLI, L., TARALLO, A., ALLCOCK, A. L. & FIORITO, G. 2021. Cerebrotypes in  
787 cephalopods: Brain diversity and its correlation with species habits, life history, and  
788 physiological adaptations. *Front Neuroanat*, 14, 565109.

789 REITER, S., HULSDUNK, P., WOO, T., LAUTERBACH, M. A., EBERLE, J. S., AKAY, L. A., LONGO, A.,  
790 MEIER-CREDO, J., KRETSCHMER, F., LANGER, J. D., KASCHUBE, M. & LAURENT, G. 2018.  
791 Elucidating the control and development of skin patterning in cuttlefish. *Nature*, 562, 361-  
792 366.

793 SANDERS, F. & YOUNG, J. 1940. Learning and other functions of the higher nervous centres of *Sepia*.  
794 *J Neurophysiol*, 3, 501-526.

795 SCHINDELIN, J., ARGANDA-CARRERAS, I., FRISE, E., KAYNIG, V., LONGAIR, M., PIETZSCH, T., PREIBISCH,  
796 S., RUEDEN, C., SAALFELD, S., SCHMID, B., TINEVEZ, J. Y., WHITE, D. J., HARTENSTEIN, V.,

797 ELICEIRI, K., TOMANCAK, P. & CARDONA, A. 2012. Fiji: an open-source platform for  
798 biological-image analysis. *Nat Methods*, 9, 676-82.

799 SCHNELL, A. K., BOECKLE, M., RIVERA, M., CLAYTON, N. S. & HANLON, R. T. 2021a. Cuttlefish exert  
800 self-control in a delay of gratification task. *Proc Biol Sci*, 288, 20203161.

801 SCHNELL, A. K., CLAYTON, N. S., HANLON, R. T. & JOZET-ALVES, C. 2021b. Episodic-like memory is  
802 preserved with age in cuttlefish. *Proc Biol Sci*, 288, 20211052.

803 SCHNELL, A. K., JOZET-ALVES, C., HALL, K. C., RADDAY, L. & HANLON, R. T. 2019. Fighting and mating  
804 success in giant Australian cuttlefish is influenced by behavioural lateralization. *Proc Biol Sci*,  
805 286, 20182507.

806 SHERRARD, K. M. 2000. Cuttlebone morphology limits habitat depth in eleven species of *Sepia*  
807 (Cephalopoda: Sepiidae). *Biol Bull*, 198, 404-14.

808 STRUGNELL, J., JACKSON, J., DRUMMOND, A. J. & COOPER, A. 2006. Divergence time estimates for  
809 major cephalopod groups: evidence from multiple genes. *Cladistics*, 22, 89-96.

810 SWEENEY, A. M., HADDOCK, S. H. & JOHNSEN, S. 2007. Comparative visual acuity of coleoid  
811 cephalopods. *Integr Comp Biol*, 47, 808-814.

812 TOMPSETT, D. H. 1939. *Sepia. LMBC Memoirs on typical British marine plants and animals*, XXXII.

813 TOURNIER, J. D., SMITH, R., RAFFELT, D., TABBARA, R., DHOLLANDER, T., PIETSCH, M., CHRISTIAENS,  
814 D., JEURISSEN, B., YEH, C. H. & CONNELLY, A. 2019. MRtrix3: A fast, flexible and open  
815 software framework for medical image processing and visualisation. *Neuroimage*, 202,  
816 116137.

817 WAGNER, H. J. 2001. Sensory brain areas in mesopelagic fishes. *Brain Behav Evolut*, 57, 117-133.

818 WILD, E., WOLLESEN, T., HASZPRUNAR, G. & HESS, M. 2015. Comparative 3D microanatomy and  
819 histology of the eyes and central nervous systems in coleoid cephalopod hatchlings. *Org  
820 Divers Evol*, 15, 37-64.

821 WILLIAMSON, R. & CHRACHRI, A. 2004. Cephalopod neural networks. *Neurosignals*, 13, 87-98.

822 WOLFF, G. H., THOEN, H. H., MARSHALL, J., SAYRE, M. E. & STRAUSFELD, N. J. 2017. An insect-like  
823 mushroom body in a crustacean brain. *eLife*, 6, e29889.

824 YANG, T. I. & CHIAO, C. C. 2016. Number sense and state-dependent valuation in cuttlefish. *Proc Biol  
825 Sci*, 283, 20161379.

826 YASUMURO, H., NAKATSURU, S. & IKEDA, Y. 2015. Cuttlefish can school in the field. *Marine Biology*,  
827 162, 763-771.

828 YOPAK, K. E., LISNEY, T. J. & COLLIN, S. P. 2015. Not all sharks are "swimming noses": variation in  
829 olfactory bulb size in cartilaginous fishes. *Brain Struct Funct*, 220, 1127-43.

830 YOPAK, K. E., LISNEY, T. J., DARLINGTON, R. B., COLLIN, S. P., MONTGOMERY, J. C. & FINLAY, B. L.  
831 2010. A conserved pattern of brain scaling from sharks to primates. *Proc Natl Acad Sci U S A*,  
832 107, 12946-12951.

833 YOPAK, K. E., PAKAN, J. M. P. & WYLIE, D. 2020. The cerebellum of nonmammalian vertebrates. In:  
834 KAAS, J. H. (ed.) *Evolutionary Neuroscience*. London: Academic Press.

835 YOUNG, J. Z. 1971. *The anatomy of the nervous system of Octopus vulgaris*, Oxford,, Clarendon Press.

836 YOUNG, J. Z. 1974. The central nervous system of *Loligo*. I. The optic lobe. *Philos Trans R Soc Lond B  
837 Biol Sci*, 267, 263-302.

838 YOUNG, J. Z. 1976. The nervous system of *Loligo*. II. Subesophageal centers. *Philos Trans R Soc Lond  
839 B Biol Sci*, 274, 101-167.

840 YOUNG, J. Z. 1977. The nervous system of *Loligo*. III. Higher motor centers - The basal  
841 supraesophageal lobes. *Philos Trans R Soc Lond B Biol Sci*, 276, 351-398.

842 YOUNG, J. Z. 1979. The nervous system of *Loligo*. V. The vertical lobe complex. *Philos Trans R Soc  
843 Lond B Biol Sci*, 285, 311-354.

844 YUSHKEVICH, P. A., PIVEN, J., HAZLETT, H. C., SMITH, R. G., HO, S., GEE, J. C. & GERIG, G. 2006. User-  
845 guided 3D active contour segmentation of anatomical structures: Significantly improved  
846 efficiency and reliability. *NeuroImage*, 31, 1116-1128.

847 ZIADI-KUNZLI, F., IGLESIAS, T., LAJBNER, Z., GUTNICK, T., MILLER, J. & KUBA, M. 2019. Quantitative  
848 analysis of the central nervous system in a coleoid cephalopod through 3D microCT.

849 ZIEGLER, A., BOCK, C., KETTEN, D. R., MAIR, R. W., MUELLER, S., NAGELMANN, N., PRACHT, E. D. &  
850 SCHRODER, L. 2018. Digital three-dimensional imaging techniques provide new analytical  
851 pathways for malacological research. *American Malacological Bulletin*, 36, 248-273.

852 ZYLINSKI, S., DARMAILACQ, A. S. & SHASHAR, N. 2012. Visual interpolation for contour completion  
853 by the European cuttlefish (*Sepia officinalis*) and its use in dynamic camouflage. *Proc Biol Sci*,  
854 279, 2386-90.

855 ZYLINSKI, S., HOW, M. J., OSORIO, D., HANLON, R. T. & MARSHALL, N. J. 2011. To be seen or to hide:  
856 visual characteristics of body patterns for camouflage and communication in the Australian  
857 giant cuttlefish *Sepia apama*. *Am Nat*, 177, 681-690.

858

859

860

861

862

863

864

865

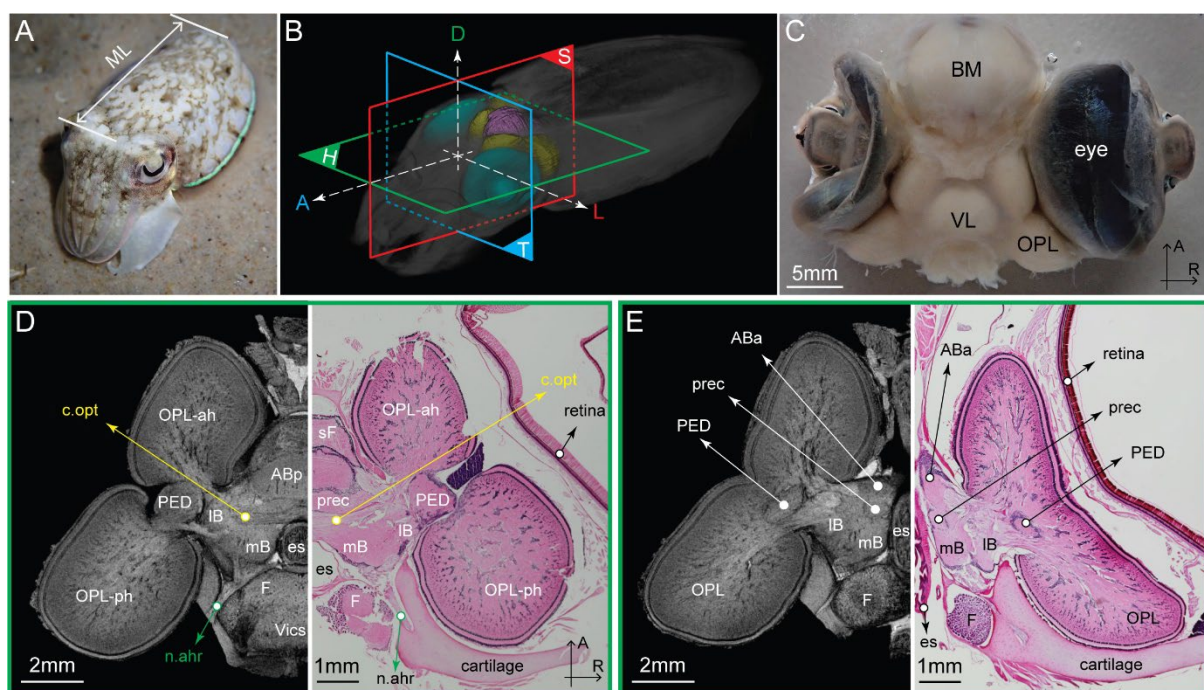
866

867

868

869

870

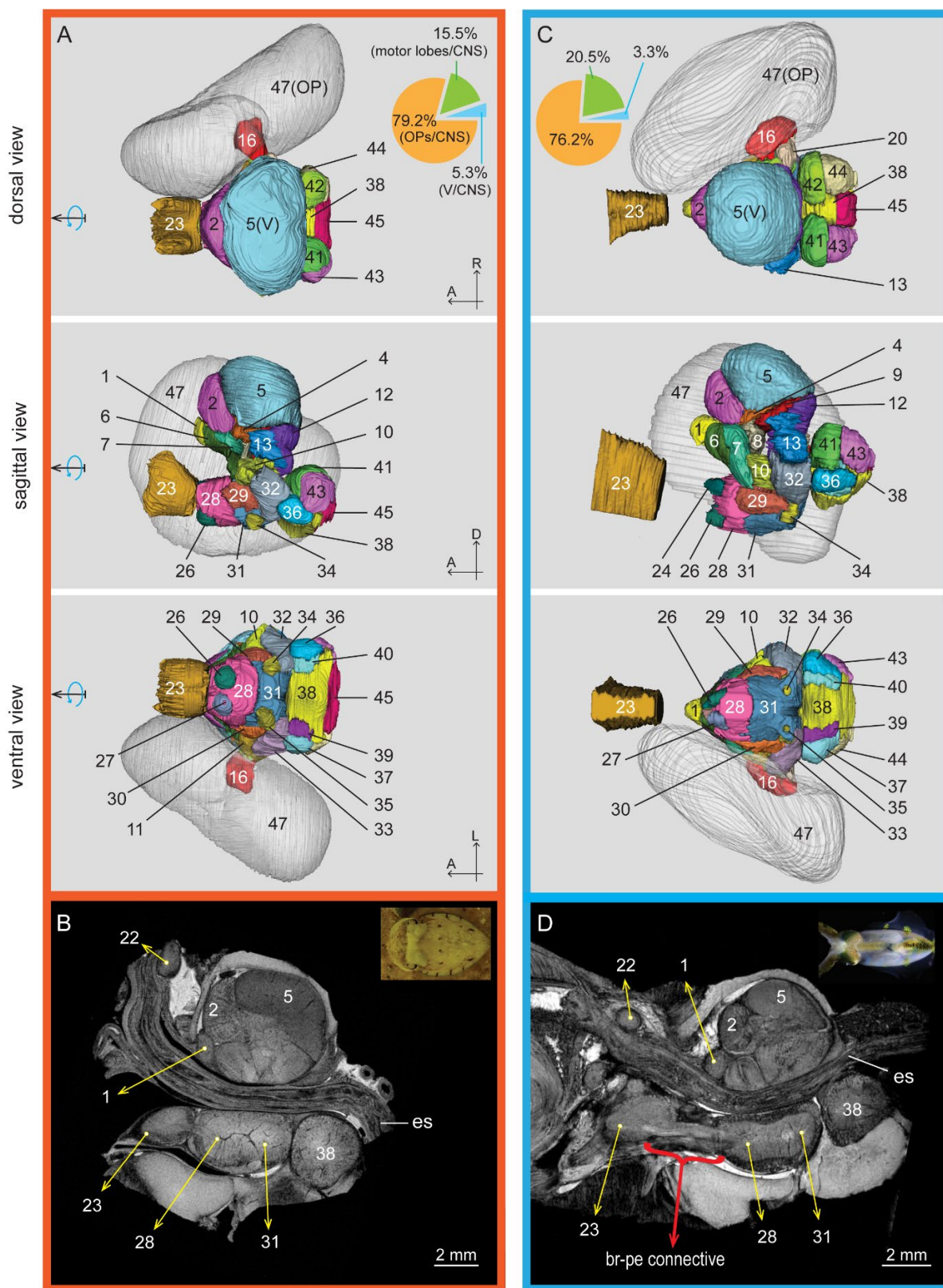


871

872

873 **Figure 1. The diurnal cuttlefish, *Sepia plangon*, and the features of its central nervous  
874 system (CNS)**

875 **(A)** Live juvenile, *S. plangon*. ML - mantle length. **(B)** Three anatomical planes and 3D MRI  
876 rendering of an entire cuttlefish and the underlying CNS and eyes. H- horizontal; S- sagittal;  
877 T- transverse plane. A - anterior; P - posterior; D - dorsal; L – left; R - right lateral side. **(C)**  
878 Isolated brain-eyes preparation (dorsal view). BM- buccal mass; OPL - optic lobe; VL-  
879 vertical lobe. **(D-E)** Comparisons of horizontal sections between magnetic resonance  
880 histology (left) (isotropic resolution 30  $\mu$ m) and conventional histology (right) (10  $\mu$ m slice  
881 stained with hematoxylin and eosin). es- esophagus; Anterior anterior basal lobe (aBa);  
882 anterior posterior basal (aBp); optic connective (c.opt); anterior head retractor nerve (n.ahr);  
883 superior frontal (sF); lateral basal (IB); median basal (mB); precommisural (prec); peduncle  
884 (PED); fin (F); visceral (Vics); anterior horn of optic lobe (OPL-ah); posterior horn of optic  
885 lobe (OPL-ph).



886

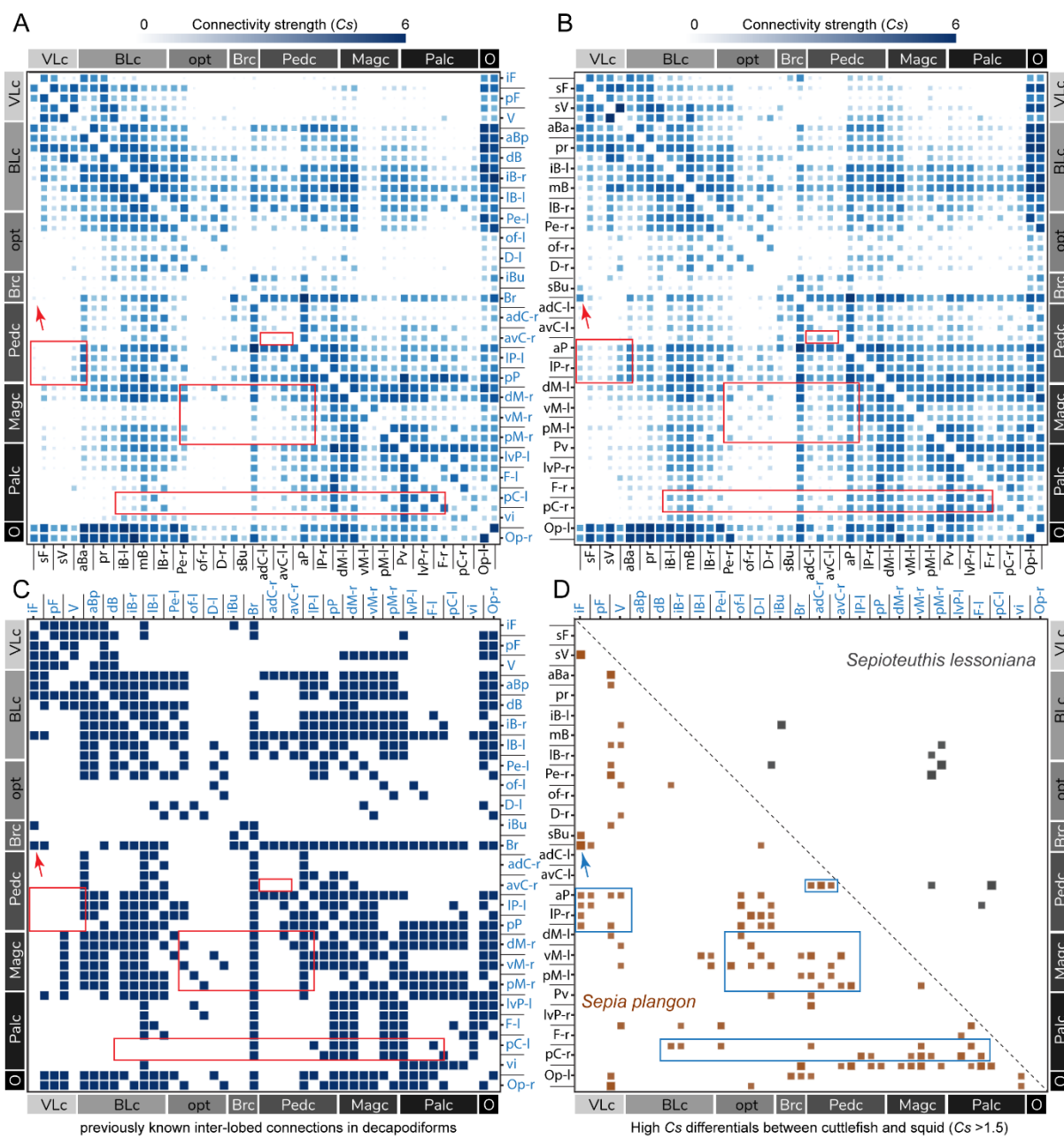
887

888

889 **Figure 2 MRI-based 3D reconstruction of two types of decapodiform multi-lobed brains**  
890 (Top, middle and bottom rows are dorsal, sagittal, ventral viewpoints and sagittal section  
891 along the central midline).

892 CNS gross anatomy and lobe organisation are superficially similar between cuttlefish and  
893 squid. **(A-B)** The diurnal tropical cuttlefish, *Sepia plangon*, its CNS layout and lobe-type are  
894 similar to that of the nocturnal temperate *Sepia officinalis*. **(C-D)** The reef squid *Sepioteuthis*  
895 *lessoniana* and its CNS layout. **(D)** The long brachio-pedal connective makes the squid  
896 brachial lobe further away from the pedal lobe complex, rendering an elongated sub-  
897 esophageal mass compared to it of the cuttlefish **(B)**. In total 47 lobes are identified (15 of  
898 which are bilateral) (See also Tables S1-2): (1) inferior frontal lobe; (2) superior frontal; (3)  
899 posterior frontal; (4) subvertical; (5) vertical; (6) anterior anterior basal; (7) anterior posterior  
900 basal; (8) precommissural; (9) dorsal basal (10-11) interior basal; (12) median basal; (13-14)  
901 lateral basal; (15-16) peduncle; (17-18) olfactory; (19-20) dorsolateral; (21) inferior buccal;  
902 (22) superior buccal; (23) brachial; (24-25) anterior dorsal chromatophore; (26-27) anterior  
903 ventral chromatophore; (28) anterior pedal; (29-30) lateral pedal; (31) posterior pedal; (32-33)  
904 dorsal magnocellular; (34-35) ventral magnocellular; (36-37) posterior magnocellular; (38)  
905 palliovisceral; (39-40) lateral ventral palliovisceral; (41-42) fin; (43-44) posterior  
906 chromatophore; (45) visceral; (46-47) optic.

907



923 regions show strong Cs values in cuttlefish which are related to chromatophore,  
924 magnocellular and pedal lobes where are potentially related to a large set of network in  
925 charge of complex colouration displays.

926

927

928

929

930

931

932

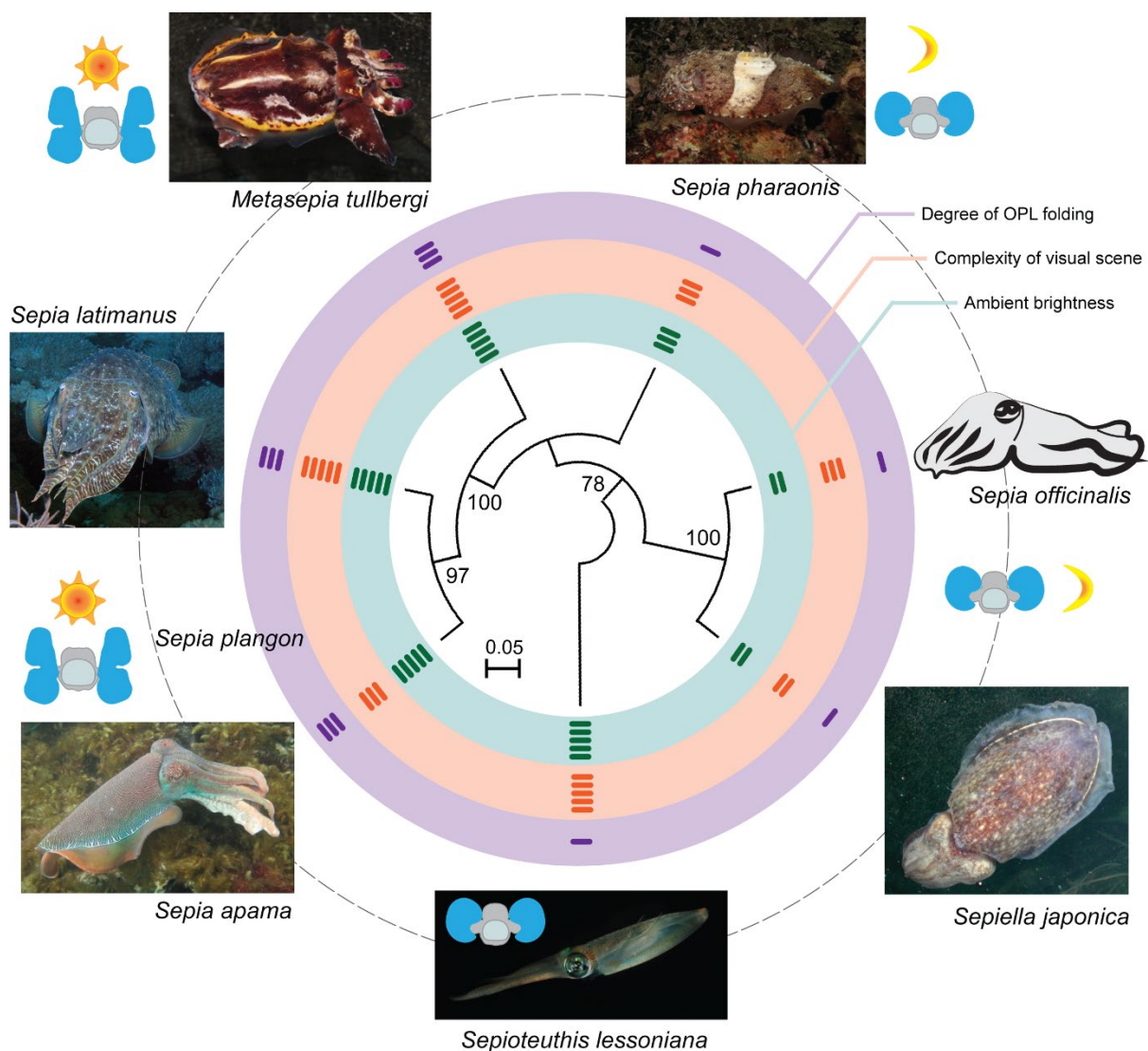
933

934

935

936

937



938

939

940 **Figure 4 Diversity of neuroanatomical features in the optic lobe (blue) of the selected 7**  
941 **decapodiforms and the corresponding life modes**

942 The phylogenetical tree in the centre is constructed based on the published molecular  
943 information (entire mitochondrial DNA sequences were available in the selected 7 species,  
944 Star Method table). Due to partially sequenced molecular data, *Sepia plangon* was excluded.  
945 The bootstrap values are shown in front of the branch node. The neuroanatomical features  
946 and corresponding habit and habitats were based on the current study and the published  
947 literature (See also Table 1). Schematic sun indicates diurnal active species; schematic  
948 moons – nocturnal active species. Coloured bars in the two inner circles (green and orange)  
949 indicate degree of complexity of the visual scene estimated by their ecological niches and the  
950 ambient brightness the species inhabits based on published literature. Dark purple bars (in the  
951 purple circle) show the degree of structural folding of the optic lobe (OPL). A similar feature  
952 of the croissant-shaped OPL described in *Sepia plangon* is found in the three diurnal species  
953 using dissection.

954

955

| Species                        | Body size<br>Mantle length or<br>total length (mm)<br>(maturity) | OPs/CNS<br>(VL/CNS)      | OP shape | Life mode  | Habitat/depth          | References  |
|--------------------------------|--|--------------------------|----------|------------|------------------------|---|
| <i>Sepia plangon</i>           | ML 71-107<br>(adults)  | 81% (4.3%)               | C        | D          | Reef (down to<br>83m)  | Current study   |
| <i>Sepia latimanus</i>         | ML 35<br>(40d post hatchling)                                    | 83% (ca2%)               | C        | D          | Reef (down to<br>30m)  | Ziadi-Kunzli et al, 2018<br>Roper et al 2005  |
| <i>Sepia bandensis</i>         | TL 80<br>(adult)   | 74% (5.1%)               | B        | N          | Reef                   | Montague et al 2022<br>Roper et al 2005   |
| <i>Sepia elegans</i>           | -  | 60% (3.2%)               | B        | -          | Down to 500 m          | Ziegler et al 2018<br>Roper et al 2005  |
| <i>Sepia officinalis</i>       | ML 80<br>(subadult)<br>-   | 67% (0.3%)<br>67% (3.7%) | B        | N          | Down to 200 m          | Wirez 1959,<br>Denton & Gilpin-Brown, 1961<br>Maddock & Young, 1987<br>Roper et al 2005 |
| <i>Sepia omani</i>             | TL 247<br>(adult)  | -/-                      | B        | -          | 50-210m                | Roper et al 2005  |
| <i>Sepia orbignyana</i>        | -  | 58% (3.3%)               | B        | -          | 15-570m                | Roper et al 2005  |
| <i>Sepia pharaonis</i>         | ML 10 - 302<br>(hatching to adult)                               | -/-                      | B        | N          | Down to 130m           | Liu et al 2017<br>Roper et al 2005  |
| <i>Sepiella japonica</i>       | -  | -/-                      | B        | -          | 50m                    | Li et al 2018<br>Roper et al 2005   |
| <i>Sepioteuthis lessoniana</i> | ML 40 - 113<br>(juvenile)  | 80% (2.6%)               | B        | cathemeral | Reef (down to<br>100m) | Chung et al 2020<br>Roper et al 2005  |

**Table 1** List of ecological, behavioural, neuroanatomical features and estimates of lobe volume of decapodiforms used in this study. B- bean-shaped; C- croissant-shaped; D- diurnal; N- nocturnal.

| Lobe system and function   | Lobe                                   | Abbreviation |
|--|--|--------------|
| Vertical lobe complex (VLC) - Memory & learning  | Inferior frontal                       | iF           |
|  | Superior frontal                       | sF           |
|  | Posterior frontal                      | pF           |
|  | Subvertical                            | sV           |
|  | Vertical                               | V            |
| Basal lobe complex (BLc) - Higher motor control  | Anterior anterior basal                | aBa          |
|  | Anterior posterior basal               | aBp          |
|  | Precommisural                          | pr           |
|  | Dorsal basal*                          | dB           |
|  | Interbasal*                            | iB           |
|  | Median basal                           | mB           |
|  | Lateral basal*                         | lB           |
| Optic track complex (opt) - Intermediate visual-motor center & olfaction                     | Peduncle*                              | Pe           |
|  | Olfactory*                             | of           |
|  | Dorsolateral*                          | D            |
| Brachial lobe complex (Brc) - Arm and feeding control  | Inferior buccal                        | iBu          |
|  | Superior buccal                        | sBu          |
|  | Brachial                               | Br           |
| Pedal lobe complex (Pedc) - Intermediate and lower motor center for locomotion control       | Anterior dorsal chromatophore* $\Psi$  | adC          |
|  | Anterior ventral chromatophore* $\Psi$ | avC          |
|  | Anterior pedal                         | aP           |
|  | Lateral pedal*                         | lP           |
|  | Posterior pedal                        | pP           |
| Magnocellular lobe complex (Magc) - Intermediate motor center                                | Dorsal magnocellular*                  | dM           |
|  | Ventral magnocellular*                 | vM           |
|  | Posterior magnocellular*               | pM           |
| Palliovisceral lobe complex (Palc) - Lower motor center for locomotion and mantle activities | Palliovisceral                         | Pv           |
|  | Lateral ventral palliovisceral*        | lvP          |
|  | Fin*                                   | F            |
|  | Posterior chromatophore*               | pC           |
|  | Visceral                               | vi           |
| Optic lobes (O) - Vision   | Optic*                                 | OPL          |

956

957 Table S1 List of cuttlefish brain lobes with abbreviations used through the text

958 The main functions of the lobe systems based on work by Young and his colleagues  
 959 (Messenger, 1979; Young, 1961, 1971; 1974, 1976; 1977, 1979; Boycott and Young, 1955,  
 960 1957; Boycott, 1961; Nixon and Young, 2003). Supraoesophageal mass includes basal lobe  
 961 and optic track complexes. Suboesophageal mass consists of the brachial lobe, pedal lobe,  
 962 magnocellular lobe, and palliovisceral lobe complexes. \* indicates that the lobe is further  
 963 divided into the left and right lobe.  $\Psi$  indicates a further sub-division of the anterior  
 964 chromatophore lobes into dorsal and ventral halves.

965

966

967

968

969

970

|                    |                         | Hatching<br>ML:8mm | Juvenile<br>ML:18mm | Juvenile<br>ML:32.4mm | Adult male<br>ML:72.9mm | Adult female<br>ML:71.1mm | Adult female<br>ML:107mm |
|--------------------|-------------------------|--------------------|---------------------|-----------------------|-------------------------|---------------------------|--------------------------|
| VL complex         | iFL                     | 1                  |                     | 0.11                  | 0.36                    | 0.39                      | 0.97                     |
|                    | sFL                     | 2                  |                     | 1.14                  | 3.56                    | 3.67                      | 8.18                     |
|                    | pFL                     | 3                  |                     | 0.16                  | 0.13                    | 0.20                      | 0.16                     |
|                    | sVL                     | 4                  |                     | 0.95                  | 3.43                    | 4.26                      | 9.04                     |
|                    | VL                      | 5                  |                     | 4.14                  | 15.62                   | 18.12                     | 46.61                    |
| ABL complex        | ABL-a                   | 6                  |                     | 0.47                  | 1.62                    | 1.91                      | 4.49                     |
|                    | ABL-p                   | 7                  |                     | 0.55                  | 1.74                    | 1.69                      | 3.56                     |
|                    | preCL                   | 8                  |                     | 1.02                  | 1.48                    | 2.41                      | 3.14                     |
| BL complex         | dBBL                    | 9                  |                     | 0.52                  | 0.62                    | 1.42                      | 2.67                     |
|                    | intBL-L                 | 10                 |                     | 0.19                  | 0.54                    | 0.81                      | 1.85                     |
|                    | intBL-R                 | 11                 |                     | 0.16                  | 0.53                    | 0.73                      | 1.93                     |
|                    | mBL                     | 12                 |                     | 1.62                  | 4.73                    | 5.07                      | 14.37                    |
|                    | IBL-L                   | 13                 |                     | 0.21                  | 1.01                    | 0.67                      | 1.21                     |
| OPT complex        | IBL-R                   | 14                 |                     | 0.21                  | 1.01                    | 0.63                      | 1.45                     |
|                    | PeduncleL               | 15                 |                     | 0.31                  | 1.00                    | 1.32                      | 2.54                     |
|                    | PeduncleR               | 16                 |                     | 0.36                  | 0.99                    | 1.20                      | 2.54                     |
|                    | ofL-L                   | 17                 |                     | 0.06                  | 0.17                    | 0.29                      | 0.05                     |
|                    | ofL-R                   | 18                 |                     | 0.05                  | 0.17                    | 0.31                      | 0.03                     |
| BrachL complex     | DorsolatL-L             | 19                 |                     | 0.05                  | 0.16                    | 0.29                      | 0.18                     |
|                    | DorsolatL-R             | 20                 |                     | 0.05                  | 0.16                    | 0.31                      | 0.19                     |
|                    | sBuL                    | 22                 |                     | 0.22                  | 1.05                    | 1.11                      | 2.00                     |
| PedL complex       | Brachil                 | 23                 |                     | 0.87                  | 5.45                    | 6.40                      | 12.21                    |
|                    | Chrom-dA-L              | 24                 |                     | 0.08                  | 0.31                    | 0.32                      | 0.28                     |
|                    | Chrom-dA-R              | 25                 |                     | 0.08                  | 0.32                    | 0.31                      | 0.29                     |
|                    | Chrom-vA-L              | 26                 |                     | 0.09                  | 0.32                    | 0.26                      | 0.48                     |
|                    | Chrom-vA-R              | 27                 |                     | 0.08                  | 0.30                    | 0.29                      | 0.40                     |
|                    | Pedal-a                 | 28                 |                     | 1.18                  | 3.59                    | 3.98                      | 10.82                    |
|                    | Pedal-l-L               | 29                 |                     | 0.32                  | 0.93                    | 0.94                      | 0.98                     |
|                    | Pedal-l-R               | 30                 |                     | 0.36                  | 0.98                    | 0.85                      | 1.00                     |
|                    | Pedal-p                 | 31                 |                     | 1.43                  | 4.28                    | 5.20                      | 11.03                    |
| Magno complex      | Magno-d-L               | 32                 |                     | 0.38                  | 1.09                    | 1.52                      | 2.95                     |
|                    | Magno-d-R               | 33                 |                     | 0.38                  | 1.19                    | 1.62                      | 2.77                     |
|                    | Magno-v-L               | 34                 |                     | 0.12                  | 0.33                    | 0.30                      | 0.29                     |
|                    | Magno-v-R               | 35                 |                     | 0.12                  | 0.31                    | 0.27                      | 0.36                     |
|                    | Magno-p-L               | 36                 |                     | 0.41                  | 0.53                    | 0.91                      | 1.24                     |
| Palliovisc complex | Magno-p-R               | 37                 |                     | 0.45                  | 0.50                    | 0.85                      | 1.21                     |
|                    | PallioVis               | 38                 |                     | 1.04                  | 3.12                    | 4.46                      | 10.17                    |
|                    | PallioVis-lv-L          | 39                 |                     | 0.51                  | 0.34                    | 0.88                      | 1.21                     |
|                    | PallioVis-lv-R          | 40                 |                     | 0.50                  | 0.36                    | 0.92                      | 1.07                     |
|                    | FinL-L                  | 41                 |                     | 0.06                  | 0.47                    | 0.91                      | 2.91                     |
|                    | FinL-R                  | 42                 |                     | 0.07                  | 0.42                    | 0.95                      | 2.58                     |
|                    | Chrom-p-L               | 43                 |                     | 0.19                  | 0.14                    | 0.81                      | 1.72                     |
| Optic lobes        | Chrom-p-R               | 44                 |                     | 0.19                  | 0.16                    | 0.72                      | 1.63                     |
|                    | Visc                    | 45                 |                     | 0.16                  | 0.29                    | 1.25                      | 4.96                     |
|                    | OPL-L                   | 46                 |                     | 43.63                 | 157.50                  | 188.64                    | 334.56                   |
|                    | OPL-R                   | 47                 |                     | 46.81                 | 155.50                  | 184.37                    | 356.52                   |
|                    | CC (mm <sup>3</sup> )   | 2.15               | 7.44                | 21.75                 | 66.17                   | 82.62                     | 181.49                   |
|                    | OPLs (mm <sup>3</sup> ) | 7.11               | 28.82               | 90.44                 | 313.00                  | 373.01                    | 691.08                   |
|                    |                         | 9.26               | 36.26               | 112.19                | 379.17                  | 455.63                    | 872.57                   |

Table S2 Estimates of lobe volume of the mourning cuttlefish, *Sepia plangon*

| Species  | ML(mm) | OPLs (mm <sup>3</sup> ) | CC (mm <sup>3</sup> ) | CNS(mm <sup>3</sup> ) | VL (mm <sup>3</sup> ) | OPLs/CNS(%) | VL/CNS(%) |
|--|--------|-------------------------|-----------------------|-----------------------|-----------------------|-------------|-----------|
| <i>Sepia elegans</i>                                   | -      | 296.00                  | 197.00                | 493.00                | 15.88                 | 59.68       | 3.22      |
| <i>Sepia orbignyana</i>                                | -      | 274.00                  | 198.40                | 472.40                | 15.49                 | 57.81       | 3.28      |
| <i>Sepia officinalis</i> (H) (Wild et al 2015)         | 6.30   | 1.96                    | 0.97                  | 2.94                  | n.a.                  | 66.85       | n.a.      |
| <i>Sepia officinalis</i> (Maddock & Young 1987)        | 80.00  | 232.40                  | 163.80                | 396.20                | 1.19                  | 58.66       | 0.30      |
| <i>Sepia officinalis</i> (Wirz, 1959)                  | -      | -                       | -                     | -                     | -                     | 67.03       | 3.68      |
| <i>Sepia officinalis</i> (Frosch, 1971)                | -      | -                       | -                     | -                     | -                     | 70.73       | 2.03      |
| <i>Sepia bandensis</i> (Montague, et al 2022)          | ca. 60 | 233.24                  | 80.43                 | 313.67                | 16.05                 | 74.36       | 5.12      |
| <i>Sepia latimanus</i> (H) (Ziadi-Kunzli, et al 2019 ) | -      | -                       | -                     | -                     | -                     | ca. 82      | -         |
| <i>Sepia plangon</i> (H)                               | 8.00   | 7.11                    | 2.15                  | 9.26                  | 0.22                  | 76.78       | 2.38      |
| <i>Sepia plangon</i> (J)                               | 18.00  | 28.82                   | 7.44                  | 36.26                 | 1.41                  | 79.48       | 3.89      |
| <i>Sepia plangon</i> (J)                               | 32.00  | 90.44                   | 21.75                 | 112.19                | 4.14                  | 80.61       | 3.69      |
| <i>Sepia plangon</i> (F)                               | 71.00  | 373.00                  | 82.62                 | 455.62                | 18.12                 | 81.87       | 3.98      |
| <i>Sepia plangon</i> (M)                               | 73.00  | 313.00                  | 73.30                 | 386.30                | 15.51                 | 81.03       | 4.02      |
| <i>Sepia plangon</i> (F)                               | 107.00 | 691.00                  | 181.50                | 872.50                | 46.61                 | 79.20       | 5.34      |
| <i>Sepioteuthis lessoniana</i> (Chung et al 2020)      | 55.00  | 98.12                   | 22.89                 | 121.01                | 2.69                  | 81.08       | 2.22      |
| <i>Sepioteuthis lessoniana</i>                         | 40.30  | 112.41                  | 25.38                 | 137.79                | 3.59                  | 81.58       | 2.61      |
| <i>Sepioteuthis lessoniana</i>                         | 49.30  | 175.23                  | 41.77                 | 217.00                | 5.61                  | 80.75       | 2.59      |
| <i>Sepioteuthis lessoniana</i>                         | 58.30  | 207.70                  | 48.03                 | 255.73                | 5.65                  | 81.22       | 2.21      |
| <i>Sepioteuthis lessoniana</i>                         | 113.00 | 443.90                  | 138.48                | 582.38                | 19.07                 | 76.22       | 3.27      |

Table S3. List of estimates of brain volume in cuttlefish and squid.  
 bioRxiv preprint doi: <https://doi.org/10.1101/2022.05.19.491988>; this version posted May 19, 2022. The copyright holder for this preprint (which was not certified by peer review) is the author/funder, who has granted bioRxiv a license to display the preprint in perpetuity. It is made available under aCC-BY-NC-ND 4.0 International license.